

UT-DRO

Annual Research Day

Thursday May 9, 2019
The Estates of Sunnybrook



Radiation Oncology
UNIVERSITY OF TORONTO

Contents

Page 4 Welcome Message

Page 5 Program

Page 9 Oral Abstracts

Page 25 Poster Abstracts

Welcome Message


On behalf of the organizing committee, welcome to the University of Toronto, Department of Radiation Oncology (**UTDRO**) **Research Day 2019** at Sunnybrook Estates. We are excited to showcase the extraordinary work that our trainees in radiation oncology, medical physics, radiotherapy and basic radiation sciences are undertaking in our department. We hope that this program will initiate thoughtful dialogue and synergize new collaborations within the UTDRO clinical and academic community. This meeting is aimed to provide a cross-section of our research accomplishments together and highlight the diverse and innovative work that our trainees have been involved in over the past year.

We also welcome **Dr. Fiona Rawle** as our keynote speaker. Dr. Rawle is the Associate Dean (Undergraduate Studies) at the University of Toronto (Mississauga) and an Associate Professor in the Department of Biology. We are looking forward to gaining Dr. Rawle's insight on unconscious bias and we take this opportunity to thank her for accepting our invitation as keynote speaker.

While the scientific and clinical focus this year remains on advancing knowledge in radiation medicine, we will be highlighting four areas of research. Firstly, UTDRO faculty and trainees present their work in **artificial intelligence** (AI) which is being studied to improve radiation treatments, as well as for enhancing patient care. The second area of research involves innovations in **brachytherapy**, which has demonstrated rapid advancements with the use of image-guidance. Thirdly, our colleagues present their exciting work in **radiation biology**, demonstrating our significant contributions to basic science research. Lastly, the program includes **epidemiological and outcomes research**; here, underscoring factors associated with treatment response outcomes. Together, these ongoing projects reflect the strong and vibrant research in our department and importantly, they all share the common focus of improving the care of our patients.

Finally, we would like to extend a special thanks to our UTDRO Chair, Dr. Fei-Fei Liu as well all faculty members, and UTDRO staff for their continued support and participation. We hope that you enjoy the program!

Sincerely,



Michael Milosevic, MD, FRCPC
Professor and Vice-Chair, Research



William T. Tran, MRT(T), MSc, PhD
Assistant Professor

Program

12:00 – 12:30	Registration & Lunch		
12:30 – 12:40	Welcome Remarks – Dr. Fei-Fei Liu, Chair		
12:40 – 1:25	Keynote Speaker: Dr. Fiona Rawle, Ph.D “Unconscious Bias and Medicine: Key Concepts For Both Residents And Patients”		
1:25 – 1:53	Oral Presentations – Section 1: Artificial Intelligence (Moderator: Ms. Lori Holden)		
Time	#	Abstract Title	Presenter
1:25 – 1:32	1	Machine Learning-Based Method For Peer Review Rounds Case Prioritization	Leigh Conroy
1:32 - 1:39	2	Characterization Of Real Time Three-Dimensional Intra-Fraction Motion Of Stereotactic Radiosurgery (SRS) Patients With Thermoplastic Mask Immobilization	Lee MacDonald
1:39 - 1:46	3	Analysis Of Quantitative Thermal Imaging Features And Grey-Level Co-Occurrence Matrix To Predict The Onset Of Radiation- Induced Skin Toxicity	Mateusz Bielecki
1:46 – 1:53	4	Commissioning Varian’s Smart Adapt For Clinical Applications In Adaptive Radiation Therapy	Jason Vickress
1:53 – 2:03	Rapid Fire Presentations 1 - Posters #1-7 (Moderator: Dr. Jennifer Croke)		
2:03 – 2:33	Break & Poster Viewing		
2:33 – 3:01	Oral Presentations – Section 2: Biology & Imaging (Moderator: Dr. Hans Chung)		
Time	#	Abstract Title	Presenter
2:33 - 2:40	5	Preliminary Results Of A Two Stage Phase II Study Of 18F-DCFPyL PET-MR For Enabling Oligometastases Ablative Therapy In Subclinical Prostate Cancer	Rachel Glicksman
2:40 - 2:47	6	Investigation Of circRNA In Cancer	Sujun Chen
2:47 - 2:54	7	Cine MRI-Based Analysis Of Intrafractional Motion In Radiation Treatment Planning Of Head And Neck Cancer Patients	Yonatan Weiss
2:54 – 3:01	8	RNF168 Deficiency Confers Synthetic Lethality To BRCA1/2-Mutant Tumors Through Impairment Of R-Loop Resolution	Parasvi Patel

3:01 – 3:11	Rapid Fire Presentations 2 - Posters #8-14 (Moderator: Ms. Laura D'Alimonte)		
3:11 - 3:32	Oral Presentations – Section 3: Brachytherapy (Moderator: Dr. John Cho)		
Time	#	Abstract Title	Presenter
3:11 – 3:18	9	Acute And Late Genitourinary Toxicity Among Patients Receiving Vaginal High Dose Rate Interstitial Brachytherapy.	Adrian Cozma
3:18 – 3:25	10	Automated Catheter Reconstruction For TRUS HDR Prostate Brachytherapy	Joel Beaudry
3:25 – 3:32	11	MRI-Guided Focal Salvage HDR Brachytherapy For Locally Recurrent Prostate Cancer	Lisa Joseph
3:32 – 4:02	Break & Poster Viewing		
4:02 - 4:37	Oral Presentations – Section 4: Outcomes (Moderator: Dr. Kathy Han)		
Time	#	Abstract Title	Presenter
4:02 - 4:09	12	Impact Of Compliance On Outcomes For Patients On Active Surveillance For Prostate Cancer	Jay Detsky
4:09 - 4:16	13	Patterns Of Recurrence And Predictors Of Survival In Breast Cancer Patients Treated With Neoadjuvant Chemotherapy, Surgery, And Radiation	Dana Keilty
4:16 - 4:23	14	Predictors Of Leptomeningeal Disease After Hypofractionated Stereotactic Radiotherapy For Intact And Resected Brain Metastases	Timothy Nguyen
4:23 - 4:30	15	Does A Rocky Treatment Course In Head & Neck Cancer Patients Predict Oncologic Outcomes?	Nauman Malik
4:30 – 4:37	16	Radiomic Signature Using Second Order Texture Derivatives From Quantitative Ultrasound In Predicting Recurrence For Patients With Locally Advanced Breast Cancer	Archya Dasgupta
4:40 – 5:00	Closing Remarks – Dr. Mike Milosevic		
5:00 – 6:00	Wine & Cheese Social		

Poster List

Poster Number	Abstract Title	Presenter
1 – Rapid Fire	FOXO1 Inhibition As A Therapeutic Strategy For Radiation Fibrosis	Pamela Psarianos
2 – Rapid Fire	Serum Cytokine Profiling As A Potential Biomarker In Intermediate Risk Prostate Cancer: An Exploratory Study	Aruz Mesci
3 – Rapid Fire	Radiation-Induced, Hypoxia-Dependent Upregulation Of CXCL12/CXCR4 Signaling In Cervical Cancer	Meetakshi Gupta
4 – Rapid Fire	Survival Outcomes And Toxicity Of Brachytherapy Versus External Beam Boost In The Treatment Of Localized Prostate Cancer: A Systematic Review And Meta-Analysis	Jenna Adleman
5 – Rapid Fire	Evaluation Of Dosimetric Predictors Of Acute And Late Toxicity After IMRT with Concurrent Chemotherapy For Anal Cancer.	Jelena Lukovic
6 – Rapid Fire	Opioid Consumption And Pain In Gynecological Cancer Patients That Underwent Spinal Anesthesia For Interstitial Brachytherapy	Gordon Locke
7 – Rapid Fire	Dosimetric Impact Of Daily Plan Adaptation For Magnetic Resonance-Guided Liver Stereotactic Body Radiotherapy	Edward Taylor
8 – Rapid Fire	Outcomes Of Oral Cavity Squamous Cell Carcinoma Patients Under The Age Of 40 Years: A Propensity Score Matched Analysis	Astrid Billfalk-Kelly
9 – Rapid Fire	Response And Intervention To Elevated ESAS Scores: A Chart Audit Of Gynecologic Oncology Clinics	Soha Atallah
10 – Rapid Fire	Treatment Outcomes And Survival Following Definitive (Chemo) Radiotherapy In HPV+ Oropharynx Cancer: Largescale Comparison Of Two Population Based Cohorts	Pernille Lassen
11 – Rapid Fire	Targeting Ros Metabolism In Pancreatic Cancer In Combination With Radiation Therapy	Pallavi Jain
12 – Rapid Fire	Construction And Evaluation Of Novel Water Calorimeter For Use In An MR-LINAC	Mark D'Souza
13 – Rapid Fire	Assessment Of TAK-243 As A Novel Therapeutic For Small Cell Lung Cancer.	Safa Majeed
14 – Rapid Fire	Targeting Epigenetic Mechanisms As Potential Radiosensitizers In Small Cell Lung Cancer	Mansi Aparnathi
15	Evaluation Of Partial Breast Irradiation Suitability In Early Stage Breast Cancer Patients	Gemma Corey
16	A Retrospective Study Comparing The Allocation Of The Resources; Time, Money And Human Resource, Used For Stereotactic Radiosurgery And Whole Brain Radiation Therapy Treatment For Palliative Brain Metastases Patient At Carlo Fidani Peel Regional Cancer Center.	Nawroz Fatima
17	A Retrospective Study To Determine The Efficacy Of Deep Inspiration Breath-Hold On Liver Dose And Define The Liver Dose Constraints	Farimah Hadjiloei
18	A Survey Based Study Of Brain Metastases Management For Patients With Non-Small Cell Lung Cancers Or Melanoma.	Chin Heng Fong
19	Evaluation Of Multiparametric Magnetic Resonance Imaging Dose Painting To Dominant Intraprostatic Lesion In Prostate HDR Brachytherapy	Yannie Lai

20	Quantification Of Ionization Chamber Response In 1.5 T Magnetic Field With 7 MV FFF Beam	Viktor Iakovenko
21	Synthesis And Modelling The Effects Of Dose Deposition Of The Palladium Core And Gold Shell Nanoparticle For Brachytherapy	Jason Lee
22	Normal Tissue Reproducibility Using Abdominal Compression Evaluated With Magnetic Resonance Imaging	Maureen Lee
23	Single- Institution Contemporary Results Of Stage IIIA Non-Small Cell Lung Cancer (NSCLC) Treated With Radiotherapy	Youquan Li
24	Features Of Patients Living Less Than 3 Months Following Spine Stereotactic Body Radiotherapy	Kang Liang Zeng
25	A Multicenter Analysis Of The Utility Of MRI Based ADC Image Sets In Delineating GTVres Volumes In Cervical Brachytherapy	Kevin Martell
26	Stereotactic Ablative Radiotherapy For Mediastinal Lymphadenopathy: A Systematic Review	Michael Tjong
27	Well-Med: A Multidisciplinary Approach To Supporting Radiation Oncology Resident Wellness.	Indu Voruganti
28	Inter-Observer Variabilities In Applicator Reconstruction And The Dosimetric Impact In HDR Gynecological Brachytherapy	Roja Zakariaee

O1

Machine Learning-Based Method For Peer Review Rounds Case Prioritization

Leigh Conroy, Chris McIntosh, Tom Purdie

Purpose

The goal of radiation therapy (RT) peer review rounds is to identify errors, reduce treatment variation, and ensure plan quality and safety. The ability to assess all cases in a peer review setting is impeded by high workloads and increasing plan complexity. The purpose of this study was to evaluate the ability of a machine learning (ML)-based method to triage RT plans of high complexity and/or with errors for peer review prioritization.

Methods

We assigned binary planning complexity scores to 202 breast RT plans during weekly peer review rounds over 15 consecutive weeks from August to November 2018. Assigned scores were based on whether the treatment plan elicited discussion (1, outlier, n=38) or not (0, normal, n=164) during rounds. An isolation forest algorithm was trained on over 3,000 previously clinically-approved breast RT plans using engineered and learned features of the CT image, delineated regions of interest, dose distribution, and the plan including beams. The 202 scored RT plans were used as an

independent testing set to evaluate the ability to detect complex plans that prompted discussion during peer review.

Results

All RT plans were assigned a complexity score between 0 and 1 by the ML algorithm, where higher scores indicated plans with greater deviations from the training set. The area under the curve (AUC) was 0.63 with a 95% confidence interval of [0.51, 0.74]. Misclassified plans were investigated to determine the strengths and pitfalls of the method for future feature and data tuning.

Conclusion

This machine-learning based method has the potential to improve the efficiency of peer review by augmenting human discussion through case prioritization. Ongoing work to improve performance of this framework includes the addition of clinical features such as margins and grade, and the development of interpretable non-binary scores to reflect degree of complexity for case ranking.

O2

Characterization Of Real Time Three-Dimensional Intra-Fraction Motion Of Stereotactic Radiosurgery (SRS) Patients With Thermoplastic Mask Immobilization

Lee MacDonald, Jannie Schasfoort, Arjun Sahgal, Young Lee, Mark Ruschin

Purpose

The transition of brain stereotactic radiosurgery (SRS) towards non-invasive immobilization devices, such as thermoplastic masks, requires real-time monitoring during treatment to ensure accurate delivery. One issue is determining the motion threshold to pause delivery: a high threshold may render treatments inaccurate whereas a low threshold may increase the number of pauses and extend treatment time. The purpose of the present study is to statistically characterize real-time motion traces in a large cohort of patients to develop evidence-based tolerances and patient-specific predictions of tolerance violations.

Methods

SRS patients treated on the Gamma Knife Icon (GKI) were immobilized using a thermoplastic mask. An infrared motion monitor (IFMM) marker was fixed to the patients' nose and continuously monitored at 20Hz, gating the treatment at excursions from baseline exceeding 1.5 mm (treatment interruption). The traces of 462 unique patients (932 individual treatments) were collected and analyzed according to magnitude, direction of displacement, and the dependence of stability on treatment time. Treatment interruptions were analyzed to examine their directional distribution and predictability. A neural network (NN) model was developed based on a training data set of 400 traces to predict interruptions based on a subset of trace data. The model was tested on a set of 62 independent traces.

Results

The average displacement of the IFMM from baseline was 0.62 ± 0.25 mm with beam gating corrections to persistent excursions, compared to 0.96 ± 0.96 mm without corrections. Of all fractions treated, 29% incurred at least one interruption and 18% incurred two or more. 50% of first interruptions occurred within 16 minutes whereas 50% and 90% of second interruptions occurred by 27 minutes and 50 minutes, respectively. In 72% of the treatment interruptions, the Z-axis (superior-inferior) was the largest contribution to excursion. Baseline corrections significantly decreased the magnitude of motion in all three dimensions ($p < 0.01$). The NN prediction model was able to identify with 84% sensitivity whether a patient would exceed tolerance during treatment based on that patient's initial 10 minutes of treatment.

Conclusion

The IFMM provides the ability to monitor a point as a surrogate of patient intra-fraction motion and to re-localize the target volume during detected persistent excursions. Corrections to marker position significantly decrease IFMM excursions from baseline in all three axes compared to single CBCT alignment and potentially minimize deterioration plan quality from the dosimetric impact of uncorrected patient intra-fraction motion. The steady increase in interruption rate observed as treatment time increases up to 50 minutes motivates the need to try and minimize treatment time as much as possible for patient tolerability.

O3

Analysis Of Quantitative Thermal Imaging Features And Grey-Level Co-Occurrence Matrix To Predict The Onset Of Radiation- Induced Skin Toxicity

Mateusz Bielecki, Victor Lin, William Tran

Purpose

Radiation induced skin reactions occur in 90% of all breast cancer patients. Current standards of assessment are qualitative and have a high degree of inter-user variability. The use of radiomics, specifically through texture analysis, is a novel way of extracting quantitative imaging biomarkers that can be used clinically. The aim of this study was to analyze thermal imaging markers associated with the onset of radiation induced skin reactions in breast radiation therapy.

Methods

Patients (n=63) were enrolled into the study. All patients underwent adjuvant radiotherapy following either, breast conserving surgery or total mastectomy. Quantitative thermal images of the treated breast were captured using a commercially available thermal imaging camera (FLIR Radars Inc, Burlington, Canada). Thermal images of the treated and contralateral breast were taken once per week for the duration of treatment, including a baseline taken prior to starting radiotherapy. The treatment volumes were contoured using dosimetric skin renderings onto the thermal images of both breasts. Temperature (Centigrade) were extracted from a defined region of interest (ROI) using a custom-built software (MATLAB, Natick, USA). Temperatures of the ipsilateral breast were normalized to the contralateral breast at each time interval (ΔT_n). Second-order texture analyses were carried out; specifically using a Grey-Level Co-occurrence Matrix to identify thermal heterogeneity and possible biomarkers associated with skin toxicity within the ROI. Statistical analyses were carried out, which

included a one-way repeated measures ANOVA to evaluate the changes in thermal parameters over time. Additionally, predictive modeling and machine learning were used to evaluate the association with thermal features at early-treatment intervals with the final toxicity outcomes.

Results

There were significant differences in the normalized temperature (ΔT_n) between patients who demonstrated a CTCAE score ≥ 3 versus CTCAE score < 2 at the following time intervals: Before RT (CTCAE score ≥ 3 ; $\Delta T_n = 0.807^\circ\text{C} \pm 0.11^\circ\text{C}$ versus CTCAE score < 2 ; $\Delta T_n = 0.300^\circ\text{C} \pm 0.07^\circ\text{C}$; $p < 0.01$) and after three weeks of RT (CTCAE score ≥ 3 ; $\Delta T_n = 0.807^\circ\text{C} \pm 0.11^\circ\text{C}$ versus CTCAE score < 2 ; $\Delta T_n = 0.300^\circ\text{C} \pm 0.07^\circ\text{C}$; $p < 0.01$). Both patient groups (CTCAE score ≥ 3 and CTCAE score < 2) demonstrated a significant increase in the normalized temperature of the ipsilateral breast during the treatment course. The GLCM textural features did not demonstrate any significant differences between groups and did not demonstrate a significant predictive value for acute radiation dermatitis. Machine learning using a k-NN classifier was able to predict acute radiation dermatitis using the baseline univariable thermal feature, ΔT_n . The area under the curve (AUC) was 0.764, Sensitivity of 71.2% and Specificity of 78.4%.

Conclusion

Thermography biomarkers demonstrate an association to the onset of radiation induced skin reactions in patients undergoing breast cancer radiation therapy.

O4

Commissioning Varian's SmartAdapt For Clinical Applications In Adaptive Radiation Therapy

Jason Vickress, Hossein Afsharpour, Alejandra Rangel-Baltazar

Purpose

Deformable image registration (DIR) has become a necessity for any robust adaptive radiation therapy program. However, a routine clinical implementation has always been accompanied with some concerns about the accuracy of the DIR. The purpose of this work is to evaluate the DIR within SmartAdapt located in the eclipse treatment planning system from Varian, for thoracic cancer patients. Our focus is on CT to CT and CT to PET-CT deformation for the accuracy of targeting, ease of contouring and accurate dose accumulation between different image sets. Currently there is no comprehensive evaluation of this DIR algorithm in the literature.

Methods

To determine the target registration error (TRE) Ten landmarked 4DCT patients from dir-labs (www.dir-lab.com) were used. Each of the 10 4DCT images contained 300 landmarks per study matching the inhalation and exhalation phase images, providing a ground truth for the TRE. For each landmark in the inhalation phase image, the DIR was used to find its corresponding point in the exhalation phase, and the TRE was calculated as the distance between the DIR predicted point in the exhalation phase image, and the landmarked point. To study contour propagation accuracy, 20 patients were selected from our own database. Each patient contained an original planning CT (PCT) and a repeat CT (ReCT) performed after anatomy change was observed. Contours were propagated from PCT to ReCT using the DIR tool in SmartAdapt and the

results were compared to the manual contours using a DICE similarity coefficient. The contours evaluated included left and right lung (N=21), heart (N=20), esophagus (N=17) and spinal canal (N=20).

Results

The overall average TRE (including all 10 cases) was 1.3 mm with individual studies having average TRE's ranging between 0.7 and 2.1 mm. The original published results using this data set and the dir-labs own DIR algorithm (PMB 2009) reported a significantly larger error with an average TRE of 1.9 mm. For contour propagation accuracy the DICE coefficient results for left lung, right lung, heart, esophagus and spinal canal were respectively 0.93, 0.94, 0.90, 0.61, and 0.82 using DIR. Whereas the DICE was 0.89, 0.87, 0.86, 0.54, and 0.76 respectively for those organs using only rigid registration. SmartAdapt enabled contour propagation to be performed in less than 1 minute much faster compared to manual contouring.

Conclusion

Our results show that for our thoracic CT studies, SmartAdapt demonstrated an average target registration error lower than 2 mm (less than the voxel size) and an acceptable level of contour propagation accuracy. These results demonstrate the validity of the DIR algorithm in SmartAdapt allowing CT to PET-CT deformation, contour propagation and future prospects of deformed dose accumulation within eclipse.

O5

Preliminary Results Of A Two Stage Phase II Study Of 18f-DCFPyL PET-MR For Enabling Oligometastases Ablative Therapy In Subclinical Prostate Cancer

Rachel Glicksman, Ur Metser, Doug Vines, Rosanna Chan, John Valliant, Peter Chung, Mary Gospodarowicz, Andrew Bayley, Charles Catton, Padraig Warde, Joelle Helou, David Green, Nathan Perlis, Neil Fleshner, Robert Hamilton, Alexandre Zlotta, Antonio Finelli, David Jaffray, Alejandro Berlin

Purpose

Despite maximal local therapies (MLT) (radical prostatectomy followed by radiotherapy [RT]), 20-30% of men will have incurable progression of prostate cancer (PC). Most recurrences in this scenario are characterized by continuous PSA rises and failure of standard imaging (bone scan [BS] and computed tomography [CT]) to detect recurrence sites. We conducted a phase II trial for men with rising PSA after MLT using 18F-DCFPyL PET-MR followed by targeted ablation of PET positive foci. We report the results of our pre-defined analysis.

Methods

Patients with rising PSA (0.4 – 3.0 ng/mL) after MLT, negative BS/CT and no prior salvage ADT were eligible. All patients underwent 18F-DCFPyL PET-MR followed by immediate PET-CT acquisition. Those with limited disease, where possible, underwent stereotactic ablative RT (SABR) or surgery. No ADT was used. The primary endpoint was biochemical response rate (complete [undetectable PSA] or partial [PSA decline \geq 50% compared to baseline]). A Simon's two stage study design was employed. Stage 1 included 12 response-evaluable patients, requiring 1 or more responses in the absence of

grade 3+ toxicities to proceed to stage 2 (additional 25 response-evaluable patients).

Results

After a median of 58 months (range 29-120) post MLT, 20 patients underwent PET-MR/CT to have 12 response-evaluable patients. Median PSA at enrollment was 1.3 ng/mL (range 0.4-2.8). Three patients had negative PET-MR/CT, while 17 had positive scans, of which 12 (60%) were amenable to response-evaluable ablation. The median number of detected lesions in those treated was 2 (range 1-5). Ten patients underwent SABR (27-30 Gy / 3 fractions) and 2 had surgery. One patient (8%) had complete and 4 (33%) had partial PSA responses at a median of 3.3 months (range 2.8-6.0) after ablation, while the remaining 7 (59%) did not have biochemical response. No grade 3+ toxicities were observed.

Conclusion

18F-DCFPyL PET/MR has high detection rates in men with rising PSA after MLT. We observed favorable early results with SABR or surgery (41% RR). Trial completion will inform if this approach offers potential for cure in an early molecularly-defined PC oligometastatic state.

O6

Investigation Of circRNA In Cancer

Sujun Chen, Vincent Huang, Xin Xu, Julie Livingstone, Fraser Soares, Jouhyun Jeon, Yong Zeng, Junjie Tony Hua, Jessica Petricca, Haiyang Guo, Miranda Wang, Fouad Yousif, Yuzhe Zhang, Nilgun Donmez, Musaddeque Ahmed, Stas Volik, Anna Lapuk, , Melvin LK Chua, Lawrence E. Heisler, Adrien Foucal, Natalie S. Fox, Michael Fraser, Vinayak Bhandari, Yu-Jia Shiah, Jiansheng Guan, Michèle Orain, Valérie Picard, H el ene Hovington, Alain Bergeron, Louis Lacombe, Yves Fradet, Bernard T etu, Stanley Liu, Felix Feng, Xue Wu, Yang W. Shao, Malgorzata A Komor, Cenk Sahinalp, Colin Collins, Youri Hoogstrate, Mark de Jong, Remond JA Fijneman, Teng Fei, Guido Jenster, Theodorus van der Kwast, Robert G. Bristow, Paul C. Boutros, HOUSHENG H. HE

Purpose

To delineate circRNA transcriptional, functional and translational landscape and regulation in cancer

Methods

We utilize multi-cohort RNA-seq and tandem mass spectrometry data, coupled with customized loss-of-function screen to delineate the transcriptional, functional and translational landscape and regulation in cancer

Results

In my analysis on RNA-seq data from the CPC-GENE (Canadian Prostate Cancer Genome Network) project, I found widespread RNA circularization in prostate cancer. The degree of aberrant circRNA production is correlated to disease progression in multiple clinical cohorts. Loss-of-function screens identified 11.3% of the screened circRNAs as essential to prostate cancer proliferation, and for 93.6% of these, their parental linear genes are not required for proliferation. Individual circRNAs can have distinct functions, with circCSNK1G3 promoting cell growth by interacting with microRNA miR-

181. Our collaborator has established a panel of radioresistant prostate cancer models. We performed total RNA-seq in the treatment naive and radiation resistant models derived from 22RV1 and DU145 after radiation treatment of different fractionation schedule. RNA samples from nuclear and cytoplasm were collected separately and treated with or without RNase-R digestion. I have identified over 20,000 high-confident circRNAs in the samples. I will compare difference in circRNA transcriptome and localization within different radioresistant models and between the parental.

Conclusion

Our study provided the first circRNA landscape in PCa and identified circRNAs associated with PCa development and progression. Our functional genomic screens generate numerous opportunities for furthering mechanistic understanding of PCa pathogenesis and progression. Our work advocate for adoption of ultra-deep RNA-Seq without poly-A selection to systematically co-interrogate both the linear and circular transcriptomes.

07

Cine MRI-Based Analysis Of Intrafractional Motion In Radiation Treatment Planning Of Head And Neck Cancer Patients

Yonatan Weiss, Lee Chin, Angus Lau, Zain Husain, Kevin Higgins, Danny Enepekides, Antoine Eskander, Ling Ho, Ian Poon, Irene Karam

Purpose

To investigate intrafractional motion of head and neck target volumes as it pertains to radiation treatment planning and to determine patient-specific planning target volume (PTV) margins.

Methods

MR-cine imaging was performed as part of an institutional workflow for radiation treatment planning in 26 head and neck cancer patients treated with curative intent to a dose of 70 Gy in 33 fractions on 1.5T MRI between 2017-2019. Dynamic MRI scans (sagittal orientation, 2x2x7 mm³ resolution), which ranged from 3-5 minutes and 900-1500 images, were acquired. Gross target volumes (GTV) were propagated on the T1 gadolinium-enhanced sagittal sequence using deformable image registration. For each tumour contour, the position of the maximum displacement along each direction in the anterior/posterior (A/P) and superior/inferior (S/I) position was recorded. Tumour displacement during deglutition and at rest was analyzed to determine average PTV margins that account for both setup error and motion.

Results

Tumour motion was quantified in 26 patients with head and neck cancer. Most common tumour sites were oropharynx (n=17), larynx (n = 6) and hypopharynx (n = 3). The mean duration for swallowing was 2.9 seconds (range 1.7-6.2 s) with a frequency of 2.0 swallows per minute (range 0.2-6.3). The maximum range of

displacements for A/P motion was 10.3 mm/9.4 mm and S/I was 12.5 mm/20.1 mm. The mean swallow had displacements A/P of 4.3 mm/3.1 mm and S/I of 4.5 mm/6.3 mm. At rest, the mean swallow displacement was A/P 2.0 mm/1.4 mm and S/I 2.1 mm/2.7 mm. Average PTV margins required for set-up error and tumour motion (swallowing included) for A/P/S/I positions were 4.4 mm/3.9 mm/5.8 mm/7.9 mm across all tumour sites, respectively. When accounting for resting motion, average PTV margins were 4.1 mm/3.6 mm/5.5 mm/7.6 mm (A/P/S/I), respectively. For a randomly chosen subset of 5 patients, patient-specific margins were generated based on their swallowing cycle, as part of a preliminary analysis. V100 for PTV70 was calculated and compared to the original plans generated with a 5 mm PTV margin. A mean drop in coverage of 2.8% (range: 1.5-4.6%) was noted.

Conclusion

The use of MR-cine in treatment planning allows for quantification of tumor motion during swallow and resting periods and should be accounted for during treatment planning. With motion considered, the derived margins exceed the commonly used 3-5 mm PTV margins employed for head and neck cancer patients with a consequent decrease in target coverage. Quantification and analysis of tumour and patient-specific PTV margins is a step towards real-time MRI guidance adaptive radiotherapy.

O8

Rnf168 Deficiency Confers Synthetic Lethality To BRCA1/2-Mutant Tumors Through Impairment Of R-Loop Resolution

Parasvi Patel, Karan Abraham, Kiran Guturi, Luis Palomero, Zahra Khan, Brandon Ho, Francesca Mateo, Otto Sanchez, Grant Brown, Brian Raught, CIMBA, Miquel Pujana, Karim Mekhail, Anne Hakem, Razq Hakem

Purpose

While germline mutations in BRCA1 and BRCA2 (BRCA1/2) considerably increase breast and ovarian cancer risk, our understanding of the molecular mechanisms that modulate this risk and the therapeutic vulnerabilities remain poorly understood. RNF168 is an E3 ubiquitin ligase which plays a crucial role in recruiting homologous recombination (HR) and non-homologous end-joining (NHEJ) proteins to double-strand breaks (DSBs). In addition, RNF168 is overexpressed in HR-defective (HRD) cancers. Therefore, we sought to investigate the role of RNF168 in maintaining genome stability in the absence of BRCA1/2.

Methods

We generated knockout-mouse models for Rnf168, Brca1, and both, and monitored them for tumor growth. Using mammary epithelial cells derived from these mice, as well as BRCA-deficient breast and ovarian cancer cell lines depleted for RNF168 and controls, we performed immunofluorescence, immunoblotting, and proliferation assays to investigate genome stability and related mechanisms. We also used genomic and transcriptomic data to investigate RNF168 status in human cancers and its role in BRCA- and HR-defective cancers. To delve deeper in to the mechanism, we employed BioID followed by mass spectrometry (MS) to identify and characterize novel interactors of RNF168. We validated putative interactors and examined their recruitment to genomic loci of interest using chromatin immunoprecipitation followed by qPCR.

Results

RNF168 is amplified and overexpressed in breast and ovarian tumors that display HRD genomic

signature. We have found a strong correlation between low expression of RNF168 and improved overall survival of patients with HRD tumors. Our in vivo data indicates that while 70% of mice with mammary-specific deletion of Brca1 develop tumors, strikingly, additional inactivation of Rnf168 significantly protects these females from mammary tumorigenesis. Furthermore, our data reveals that RNF168 depletion elevates genomic instability, thus conferring senescence in BRCA-deficient cells. Consequently, RNF168 loss impairs in vitro and in vivo growth of BRCA-deficient tumors. We have determined that R-loop accumulation, G-quadruplex (G4) stabilization, and replication stress lead to the observed genomic instability and synthetic lethality. Corroborating our BioID-MS data, we have identified R-loop and G4 resolving helicase DHX9 as a novel interactor of RNF168. Mechanistically, RNF168 loss impairs recruitment of the helicase DHX9 to R-loops, thereby abrogating R-loop resolution. In addition, RNF168 deficiency sensitizes BRCA1/2-mutant cancer cells to irradiation, PARP inhibition, and G-quadruplex-stabilizing drugs. The relevance of these findings is extended to humans by the identification of the single-nucleotide polymorphism, rs192573104, as an expression quantitative trait locus for RNF168 that decreases breast cancer risk in BRCA1-mutation carriers.

Conclusion

These data reveal dependence of BRCA1/2-defective tumors on factors that suppress R-loops and a fundamental RNF168-mediated mechanism that determines cancer development and vulnerability.

O9

Acute And Late Genitourinary Toxicity Among Patients Receiving Vaginal High Dose Rate Interstitial Brachytherapy

Adrian Cozma, Kevin Martell, Ananth Ravi, Elizabeth Barnes, Moti Paudel, Eric Leung, Amandeep Taggar

Purpose

High dose rate (HDR) interstitial brachytherapy (ISBT) is an effective modality to deliver highly conformal doses of radiation for treatment of malignancies centered within the vagina. The aim of this study was to evaluate urethral dose and its correlation to the incidence of genitourinary complications among patients undergoing vaginal ISBT.

Methods

39 patients treated with ISBT between January 2017 and April 2018 were retrospectively reviewed after REB approval. Clinical characteristics were collected from their electronic medical records and CTCAE version 5.0 was used to grade toxicity. ISBT dosimetric information was collected through review of individual treatment plans as generated in Oncentra Brachy(R). Urethral contours were retrospectively added to the structure sets using a 1cm diameter brush and dose to 0.1cc (D0.1cc), D0.2cc and D0.5cc of urethra were obtained. Then, the total (ISBT +/- EBRT) equivalent dose in 2Gy fractions (EQD2) received by HRCTV (Gy10) and OARs (Gy3) were calculated. Numerical counts (%) and medians (Inter-Quartile-Range) were used to characterize the data. Fisher's exact and the Mann-Whitney-Wilcoxon tests were used as appropriate to determine statistical significance.

Results

The median age and follow-up was 66 years (57-73) and 9.3 months (6.4-15.3). 21 (54%) patients

had endometrial, 13 (33%) had vaginal, 4 (10%) had vulvar primaries and one (3%) had metastasis from the rectum. 30 (77%) patients received external beam radiation prior to ISBT. 17 (44%) underwent a single brachytherapy insertion and 22 (56%) received two. A median of 4 (3-6) ISBT fractions were delivered to each patient and a median of 15 needles (13-17) were used. Median total EQD2 were 55.4 (46.4-72.5), 52.3 (46.0-67.1), 50.9 (45.6-62.5) Gy for Urethral D0.1cc, D0.2cc and D0.5cc respectively. Median bladder D2cc was 65.5 (46.2-75.1). 16 of 39 (41%) patients experienced any acute and 8 of 30 (27%) any late GU toxicity (9 patients did not have follow-up >6 months). 4 (10%) had grade 2 and 0 (0%) had grade 3+ acute GU toxicity. 1 (3%) patient had grade 2 and 1 (3%) had grade 3 late GU toxicity. Median urethral D0.1cc, D0.2cc and D0.5cc were 73 Gy (51.7-93.8) and 50.5 Gy (45.2-63.7; p=0.009), 69.2 Gy (48.9-87.4) and 49.6 Gy (42.7-58.4; p=0.011) and 62.9 Gy (47.9-79.6) and 48.6 Gy (39.2-55.7; p=0.015), respectively in patients with or without any CTCAE GU toxicity. Additionally, 7 (44%) patients with and 1 (4%) without GU toxicity had bladder intrusion (p=0.004). There was no significant difference in urethral dosimetry between patients experiencing and not experiencing late toxicity.

Conclusion

Urethral dose appears to predict acute genitourinary toxicity in ISBT of vaginal tumors. Further study with an expanded cohort and longer follow-up is warranted.

O10

Automated Catheter Reconstruction For TRUS HDR Prostate Brachytherapy

Joel Beaudry, Daxa Patel, Aaron Vandermeer, Cathy Neath

Purpose

Transrectal ultrasound (TRUS) imaging is used during prostate high dose rate (HDR) radiation treatment to guide the insertion of catheters through the perineum into the prostate. Following a 3D US acquisition, the catheters are manually reconstructed in the treatment planning system, defining potential dwell positions for the HDR source. Difficulties with the reconstruction can arise due to image artifacts which either mimic or hide a catheter, thereby increasing the time of treatment planning. We propose a novel approach to catheter reconstruction from TRUS images through the use of a deep convolutional neural network combined with pre- and post-processing algorithms, collectively referred to as “DeepDwell”.

Methods

Manually reconstructed catheters and TRUS images were used to train, validate, and assess the performance of the proposed method. A total of 14 prostate patient datasets (12 training, 1 validation, 1 test) were used. The architecture of the neural network in DeepDwell is based upon a common ‘U-Net’ encoder-decoder design but with several modifications influenced by other developments in the field of image segmentation. For each TRUS slice, a stack of 5 slices is used as our training input, with the adjacent slices adding in extra spatial

information to produce a 2.5D network architecture. The predicted output corresponds to the central slice of each stack. The loss function was a combination of a generalized dice and weighted binary cross entropy. Post-processing of the network’s output resulted in the predicted catheter position. An analysis comparing predicted to ground truth catheters was performed over all slices, evaluating centre-to-centre distance and similarity.

Results

DeepDwell was used to reconstruct predicted catheters from the test dataset. The prediction was available in under 10 seconds and the number of catheters predicted and delineated in our test dataset was 13 out of 16. Of those detected, the average dice coefficient is 0.8 ± 0.1 and the average distance is within 0.3 ± 0.1 mm from the ground truth.

Conclusion

An algorithm, DeepDwell, comprised of a neural network and computer vision processing is proposed to aid in catheter detection for prostate HDR treatments. DeepDwell is able to quickly segment a majority of the catheters in test and validation datasets suggesting that the use of machine learning can be of clinical benefit. Future work will focus on improvements of detection and clinical exploration.

O11

MRI-Guided Focal Salvage HDR Brachytherapy For Locally Recurrent Prostate Cancer

Lisa Joseph, Aravind Sundaramurthy, Alejandro Berlin, Joelle Helou, Cynthia Ménard, Andrew Bayley, Charles Catton, Pdraig Warde, Bernadeth Lao, Alexandra Rink, Robert Weersink, Akbar Beiki-Ardakani, Peter Chung

Purpose

Biochemical failure may occur in up to 40% of patients treated with external beam radiotherapy (RT) alone for localized prostate cancer. A proportion of these may be associated with intraprostatic disease recurrence where further local treatment options may be limited. While efficacious, whole-gland salvage brachytherapy may be associated with significant morbidity as is the use of androgen deprivation therapy (ADT). Focal brachytherapy has recently gained more attention with the aim of avoiding morbidity associated with whole-gland brachytherapy and may facilitate deferral of ADT. We report results of a prospective study of MRI-guided focal salvage brachytherapy.

Methods

This was a phase II single-arm cohort study. Eligibility was pathologically proven locally recurrent prostate cancer visible on multi-parametric MRI (mpMRI) at least 18 months after primary RT with PSA-doubling time > 6 months, without metastatic disease on conventional imaging and ECOG performance status 0-1. All patients were treated with HDR brachytherapy under MR image guidance alone. Patients received a dose of 13Gy to a partial intraprostatic tumour-bearing region, repeated 7-14 days later. The GTV was defined on mpMRI (T2-weighted, diffusion-weighted and dynamic contrast-enhanced sequences). CTV margin expansion (5 mm in all directions) was restricted to adjacent organs at risk and 2 mm beyond the prostate boundary where applicable. PTV margins of 2 mm cranio-caudally and 1mm elsewhere were then applied. No patients were given ADT. Patients were followed

with regular 6-monthly PSA, and mpMRI +/- prostate biopsy were performed after a minimum of 2 years. Toxicity was assessed using Common Terminology Criteria for Adverse Events (v4). Biochemical relapse was defined using Phoenix definition (nadir +2).

Results

A total of 29 patients (median age 71 years, range 62-85) were enrolled. Median PSA pre-salvage was 3.93 (1.68 – 14). 2 patients had Gleason 6 disease on pre-salvage biopsy, 19 with Gleason 7, 5 Gleason 8 and 3 Gleason 9. Median follow-up was 41 months (6 - 68). Median PSA nadir prior to disease recurrence was 0.54 (<0.05 – 3.32) and time to nadir was 27.3 months (7 – 66). Crude rates of biochemical control at 2 years was 83% (19/23) and 58% (8/19) at 3 years. 17 patients were eligible and agreed to post-salvage MRI and/or biopsy. Of these, 6 (35%) had localized recurrence confirmed, 4 of which were within the treated salvage volume. GU and GI symptoms (<G2) were reported in 8 and 5 of all patients respectively at 1-month follow-up. 5 reported continual GU and 2 GI symptoms of the 24 patients that had completed 1 year follow-up (<G2). All patients are currently alive, 5 have confirmed metastases and 7 are on ADT. Only 3 of the 8 patients with Gleason 8/9 disease have disease control.

Conclusion

MR-guided focal salvage brachytherapy after failure of previous RT appears to provide good local disease control in selected patients with low rates of late toxicity. Further dose escalation to the tumor may be considered but other methods for appropriate patient selection beyond PSA dynamics and Gleason score are also needed.

O12

Impact Of Compliance On Outcomes For Patients On Active Surveillance For Prostate Cancer

Jay Detsky, Alireza Fotouhi Ghiam, Laurence Klotz, Stanley Liu, Andrew Loblaw, Danny Vesprini

Purpose

Active surveillance (AS) is the standard of care for low-risk prostate cancer (PCa) to reduce the risk of overtreatment. Compliance with repeat biopsies required on AS is low. The purpose of this study is to determine the impact of compliance with biopsies on PCa-specific outcomes.

Methods

A review of a large, mature, single-institution prospective cohort of 1,275 patients on AS for PCa was performed to determine compliance rates with biopsies. Compliance with the confirmatory (1 year) biopsy was used as a surrogate for overall compliance. The primary outcomes were recurrence after treatment and the development of metastases. Time-to-event outcomes including recurrence-free survival (RFS), metastasis-free survival (MFS), cause-specific survival (CSS) and overall survival (OS) were also determined. Recurrence was defined as PSA > 0.2 after surgery, PSA > nadir + 2 after RT, subsequent treatment for progression or the development of metastases.

Results

Amongst the 1,275 patients included, 453 (36%) received treatment for their PCa, metastases were diagnosed in 36 patients (3%) and 22

patients (2%) died of PCa. Median follow up was 7.8 years. Compliance rates with biopsies at years 1, 4 and 7 were 74%, 52% and 43%. Non-compliant patients (to the confirmatory biopsy) were older than compliant patients ($p < 0.001$) but there was no difference in baseline PSA scores ($p = 0.33$) or Grade Group ($p = 0.14$). In the cohort of treated patients, non-compliance resulted in higher rates of recurrence (41% vs 26%, OR=2.0, $p = 0.001$) even after accounting for age, PSA and Grade Group. RFS over all time points was not impacted by compliance (HR=1.29, $p = 0.13$) but there was a significant difference at the 10-year time point (HR=1.44, $p = 0.03$). The risk of developing metastases was impacted by non-compliance (OR=4.1, $p < 0.001$) and Grade Group (OR=3.2, $p = 0.001$) but not by age ($p = 0.4$) or baseline PSA ($p = 0.5$). MFS was significantly affected by compliance (HR=2.4, $p = 0.03$). CSS and OS were not impacted by compliance ($p = 0.38$ and $p = 0.68$ respectively).

Conclusion

Non-compliance with the confirmatory biopsy leads to poorer oncologic outcomes including higher rates of recurrence and metastases for men on AS for PCa. Patients should be counseled about these risks when enrolling in AS and during follow-up.

O13

Patterns Of Recurrence And Predictors Of Survival In Breast Cancer Patients Treated With Neoadjuvant Chemotherapy, Surgery, And Radiation

Dana Keilty, Shirin Namini, Monali Swain, Manjula Maganti, Tulin Cil, David McCreedy, David Cescon, Eitan Amir, Rachel Fleming, Anna Marie Mulligan, Wilfred Levin, Fei-Fei Liu, Jennifer Croke, Anthony Fyles, Anne Koch*, Kathy Han*

Purpose

Neoadjuvant chemotherapy (NAC) is standard of care for locally-advanced breast cancer and is increasingly used for early-stage high-risk disease. Previous studies have shown wide variation in radiation (RT) practice and limited data on locoregional relapse (LRR) following NAC. We hypothesized a low LRR risk after treatment with modern NAC, surgery and RT, and aimed to elucidate patterns of LRR and predictors of disease-free survival (DFS) and overall survival (OS) in these patients.

Methods

Data from 416 stage II/III breast cancer patients treated with NAC, surgery and adjuvant RT at our institution between 2008 and 2015 were retrospectively reviewed. Hormone receptor (HR) and HER2 status defined molecular subtype: HR+HER2- (45%), HR-HER2+ (11%), HR+HER2+ (22%), and HR-HER2- (22%). DFS and OS rates were calculated using the Kaplan-Meier method. LRR rate was estimated using the cumulative incidence function, treating death as a competing risk. Multivariable survival analysis was performed using Cox regression.

Results

Median follow-up was 4.7 years (range 0.5 – 10.7). Median age was 48 years (range 24 - 79). Most patients had cT2/3 (75%) cN1 (62%) disease and underwent mastectomy (76%) and axillary dissection (84%). pCR was achieved in

23% of patients: 8% of HR+HER2-, 53% of HR-HER2+, 19% of HR+HER2+, and 41% of HR-HER2-subtype. All patients received adjuvant RT, most (99%) with 50 Gy in 25 fractions. Nodal RT was given to 96% of the patients: 83% axilla and supraclavicular fossa (SCF); 8.5% SCF alone; 8% axilla, SCF, and internal mammary nodes (IMN); and 0.5% SCF and IMN. There were 19 local, 17 regional, and 88 distant failures (DM). Of the 27 patients with LRR (12 HR+HER2-, 0 HR-HER2+, 6 HR+HER2+, 9 HR-HER2-), all but 4 developed DM, 13 of which were synchronous. Two developed LRR 2 months after surgery, prior to adjuvant RT. LRR could be mapped in 22 patients: most (19) recurred in the RT field (in-field); 1 in- and out-of-field; and 2 out-of-field (1 isolated IMN recurrence and 1 IMN with DM). The 5-year LRR, DFS and OS were 6.4%, 77% and 90% for the entire cohort, respectively. On multivariable analysis, HR-HER2- subtype, stage III disease and non-pCR were associated with poor DFS (HR 2.2, 95% CI 1.3-3.6, $p = 0.002$; HR 1.8, 95% CI 1.1-2.8, $p = 0.01$; HR 4.2, 95% CI 1.9-9.1, $p < 0.001$, respectively) and OS (HR 3.9, 95% CI 1.9-8.0, $p < 0.001$; HR 1.7, 95% CI 0.9-3.4, $p = 0.095$; HR 2.6, 95% CI 1.04-6.7, $p < 0.001$, respectively).

Conclusion

Breast cancer patients treated with NAC, surgery, and RT have low 5-year LRR risk. Most LRR occur in-field. HR-HER2- subtype, stage III disease, and non-pCR are associated with poor DFS and OS.

O14

Predictors Of Leptomeningeal Disease After Hypofractionated Stereotactic Radiotherapy For Intact And Resected Brain Metastases

Timothy K. Nguyen, Arjun Sahgal, Jay Detsky, Eshetu G. Atenafu, Sten Myrehaug, Chia-Lin Tseng, Zain Husain, Mark Ruschin, Young Lee, Chris Heyn, Hany Soliman

Purpose

Hypofractionated stereotactic radiotherapy (HSRT) for patients with resected or large intact brain metastases is increasing in clinical practice; however, reporting on patterns of failure, specifically leptomeningeal disease (LMD) is lacking. In this study we identify patterns of LMD and determine predictors for developing LMD in patients with intact or resected brain metastases treated with 5-fraction HSRT.

Methods

A single-institution retrospective review of a prospective database identified patients receiving HSRT for intact brain metastases or surgical cavities. Patient, tumor and treatment factors were extracted. Patterns of LMD were stratified into four groups based on their radiographic presentation: focal classical, diffuse classical, focal nodular and diffuse nodular. Univariate and multivariable analyses were conducted to determine potential predictors for developing LMD.

Results

HSRT was delivered to 320 intracranial lesions (57% intact and 43% surgical cavities) in 235 patients with a median follow-up of 13.4 months (range, 0.8 to 60 months). The most common dose regimen was 30Gy in 5 fractions (65%). Overall, the incidence of developing LMD was 19% and the most common radiographic presentation of LMD was a diffuse nodular

pattern (44%). The 6-month and 1-year rates of LMD were 7.5% and 12%, respectively. On multivariable analysis for the entire cohort, cavity lesions were statistically significant predictors of LMD compared with intact metastases (24% vs. 7%; hazard ratio=0.47; $p=0.01$). For cavities alone, radiosensitive tumors (including non-small cell lung, small cell and breast cancer) were the only statistically significant predictor of LMD ($p=0.030$), with a trend towards significance observed for increasing maximum tumor diameter ($p=0.050$). From the date of LMD diagnosis, the median overall survival (OS) for the entire cohort was 3.8 months (range, 0.2 to 20.8 months). The 6-month and 12-month OS rates were 42% and 15%, respectively. No statistically significant difference in OS was observed between the four patterns of LMD ($p=0.203$) or between nodular and classical patterns ($p=0.267$).

Conclusion

For patients treated with HSRT, surgical cavities are at increased risk of developing LMD compared to intact brain metastases. Our findings suggest that despite the ability of HSRT to safely escalate tumor dose compared with single-fraction SRS, it may still be insufficient to mitigate the heightened risk of LMD observed with surgical cavities. Further research is required to determine optimal strategies to reduce LMD rates.

O15

Does A Rocky Treatment Course In Head & Neck Cancer Patients Predict Oncologic Outcomes?

Nauman Malik, Manjula Maganti, Maurene McQuestion, Michael Tjong, Dana Keilty, Eric Monteiro, Shao Hui Huang, Raymond Woo-Jun Jang, Andrea Gomes, Joanne Pun, Jolie Ringash

Purpose

A Rocky Treatment Course (RTC) is a previously defined intermediate-term composite outcome in head and neck cancer (HNC) patients receiving radiotherapy (RT). It is a composite of six variables: patient-driven interruptions in RT \geq 1-day, incomplete RT, incomplete chemotherapy(c) (<2 cycles), >5 visits to a walk-in nursing clinic, gastrostomy tube (G-tube) dwell time \geq 90 days, and unplanned G-tube insertion (\geq 21 days after RT start). Previous work in an earlier cohort of patients showed that components of the RTC were predictive of oncologic outcomes and late toxicities. Our objective was to investigate if having a RTC predicts oncologic outcomes and late toxicities in a more recent, independent cohort of HNC patients.

Methods

A retrospective review of HNC patients receiving RT as part of curative intent treatment from September 2013 to December 2017 was conducted. A random sample of 300 patients was drawn, of whom half attended, and the other half did not attend, a pre-treatment educational class. RTC component variables, as well as detailed treatment and toxicity data, were abstracted from chart review and merged with our prospectively collected Anthology of Outcomes quality assurance tool. Univariable analyses was conducted with individual components of, and the composite RTC; and dependent variables of overall survival (OS), locoregional recurrence (LRR), locoregional

recurrence-free survival (LRFS), and unexpected grade 3 toxicity. Multivariable analysis was performed for OS and LRFS.

Results

Overall, 123/300 (41%) patients experienced a RTC. Among those with RTC, 2-year results were: OS 74%, LRR 4.2%, LRFS 73%, and unexpected grade \geq 3 toxicity 5.7%. Among those without RTC, analogous figures were: 84%, 1.7%, 84%, and 3.9%, respectively. The differences were statistically significant for OS ($p=0.033$) and LRFS ($p=0.015$), but not for LRR ($p=0.22$) or toxicity ($p=0.48$). Among RTC components, only RT interruption was associated with worse OS (OR 1.82, CI 95% 1.04 – 3.17, $p=0.035$) and LRFS (OR 1.95, CI 95% 1.13 – 3.37, $p=0.017$) on univariable analysis. On multivariable analysis, variables (HR, 95% CI, p-value) associated with worse OS were: RTC (2.08, 1.11-3.91, 0.023), ECOG performance status \geq 1 (5.11, 2.55-10.26, <0.001), N2/3 disease (2.83, 1.38-5.8, 0.0044) and treatment modality other than cRT: RT alone (3.2, 1.39 - 7.38, 0.0064), surgery with postoperative cRT (20.41, 6.99 - 59.6, <0.001), and surgery with postoperative RT (4.28, 1.72 - 10.68, 0.0018). Similar results were seen for LRFS.

Conclusion

The association of a rocky treatment course with worse oncologic outcomes in HNC has been independently validated and could be used as an intermediate outcome variable in future prospective studies.

O16

Radiomic Signature Using Second Order Texture Derivatives From Quantitative Ultrasound In Predicting Recurrence For Patients With Locally Advanced Breast Cancer

Archya Dasgupta, Lakshmanan Sannachi, Steven Brade, Karina Quiaoit, Ali Sadeghi-Naini, William Tran, Gregory Czarnota

Purpose

Previous studies have demonstrated that quantitative ultrasound (QUS) and texture biomarkers are useful tools for predicting and monitoring treatment response in breast cancer patients undergoing neoadjuvant chemotherapy (NAC). The current study was undertaken to explore if second order texture derivatives from QUS coupled with advanced machine learning can help to predict recurrence in patients with locally advanced breast cancer (LABC).

Methods

Patients with LABC receiving NAC were scanned with a 6 MHz clinical ultrasound system before starting NAC. A total of 98 patients with a minimum follow up of 2 years (or if died from disease recurrence within 2 years) were considered eligible for the study. Five QUS parametric images were obtained from ultrasound radio-frequency data within tumor regions of interest. From each QUS-image map, four different gray-level co-occurrence matrices (GLCM) based texture images (first order texture) were derived (contrast, correlation, energy, and homogeneity) using a sliding window approach. Four texture values were further derived from each QUS images (second order) leading to a total set of 84 features for classification analysis. Patients were classified into two groups based on clinical outcomes (recurrence vs. no recurrence). Machine learning algorithms based on linear discriminant (FLD)

and k-nearest-neighbors (K-NN) were used to generate classification models.

Results

The median follow up for all the patients was 59 months (range 7 to 115 months). During the study period, 31 patients had recurrences (local-regional in 3, distant in 19, and combined in 9). The K-NN resulted in best classifier indices with sensitivity, specificity, accuracy, and area under the curve (AUC) values of 94%, 52%, 81%, and 67% respectively. Using a forward feature selection method (n=4), all the features selected by the model represented second order texture derivatives. The inclusion of molecular characteristics (hormonal receptor and Her 2 status) did not result in better classifier performance. On further analysis for 31 patients with recurrent disease, the radiomic signature was able to segregate patients controlled loco-regionally from others with an accuracy of 91%.

Conclusion

This study demonstrates pre-treatment QUS radiomic signature can help in the identification of patients with LABC at higher risk for disease recurrence. It also has the potential to predict the site of recurrence which can be exploited to decide intensification of treatment regimens (local vs. systemic therapy). Future studies with the inclusion of larger number of patients can increase the classifier performance and robustness of the models.

P1

Survival Outcomes And Toxicity Of Brachytherapy Versus External Beam Boost In The Treatment Of Localized Prostate Cancer: A Systematic Review And Meta-Analysis

Jenna Adleman, Noelia Sanmamed, Rouhi Fazelzad, Jacques Raphael, Joelle Helou

Purpose

To conduct a systematic review and meta-analysis of randomized controlled trials (RCTs) to assess survival and toxicity outcomes in men with localized prostate cancer treated with external-beam radiotherapy (EBRT) versus low (LDR)- or high dose-rate (HDR) brachytherapy (BT) boost.

Methods

An experienced librarian and two independent reviewers conducted a systematic review of the literature. Five electronic databases were searched for RCTs: Ovid MEDLINE, EMBASE, Cochrane Central Registrar of Controlled Trials, Web of Science, and Epub Ahead of Print. The primary endpoint was bDFS at 5 years and the secondary endpoints were OS at 5 years, acute genitourinary (GU) and gastrointestinal (GI) toxicity and late GU and GI toxicity. Eligible RCTs reported one of our primary or secondary endpoints in patients with localized prostate cancer treated with EBRT versus BT boost. Mantel-Haenszel with random-effect models and Peto methods were used as appropriate to pool estimates for odds ratios (ORs) with 95% confidence intervals (CIs). Subgroup analyses were performed to compare outcomes for LDR versus HDR boost.

Results

The database searches identified 8,398 records. Following elimination of duplicates, 6,577 records were screened, of which 51 records were fully assessed for eligibility. Ultimately six clinical trials met criteria for inclusion in the meta-analysis, however one abstract was subsequently excluded due to insufficient data. Three trials (60%) reported bDFS, OS, and late GU/GI toxicity. Four trials (80%) reported acute GU/GI toxicity. Two trials (40%) reported occurrence of urethral stricture. The risk of bias in the included studies assessed using the Cochrane Collaboration risk of bias tool was low in four trials and unclear in one trial. Two trials (40%) used LDR for the boost. At five years, BT boost was

associated with a 58% reduction of the odds of developing a biochemical recurrence (OR 0.42; 95% CI 0.3-0.6). On subgroup analysis, both LDR (OR 0.37; 95%CI, 0.24-0.58) and HDR boost (OR 0.52; 95%CI, 0.29-0.94) were associated with better bDFS compared to EBRT with no statistically significant subgroup difference ($p=0.36$). No difference was found in terms of five-year OS between EBRT and BT boost (OR 0.83; 95% CI 0.54-1.27). There was no difference in acute GU or GI toxicity by study arm (OR 1.88; 95% CI 0.65-5.42) or by subgroup analysis for dose-rate (test for subgroup differences, $p=0.32$). Late GU toxicity was worse in the BT boost arm (OR 1.87; 95% CI 1.23-2.85). The subgroup analysis showed an increased late GU toxicity in patients treated with LDR boost versus EBRT (OR 3.31; 95% CI 1,84-5.94) while no difference was observed in patients treated with HDR boost versus EBRT (OR 1.01; 95% CI 0.55-1.86)(test for subgroup differences, $p=0.006$). Late GI toxicity was not statistically different in the BT boost arm (OR 1.85; 95% CI 0.94-3.61). Both LDR and HDR boost were not associated with an increased late GI toxicity compared to EBRT (test for subgroup differences $p=0.34$). Urethral stricture was more prevalent in the BT boost arm (OR 4.36; 95% CI 1.99-9.57). In the subgroup analysis, LDR was associated with increased odds of urethral strictures (OR 5.3; 95%CI, 2.06-13.63) while there was no difference in urethral strictures between patients treated with HDR boost versus EBRT (OR 2.84; 95%CI, 0.69-11.62).

Conclusion

Patients treated with either LDR or HDR boost had better bDFS compared to those treated with EBRT. Late GU toxicity and urethral stricture were increased in the BT boost arm particularly with LDR boost. Despite pooled data analysis, there was no significant difference in 5-year OS between the two arms. However, given the natural course of prostate cancer, 5 years is likely insufficient to detect an OS difference in this population. Longer follow-up and more events are needed to improve the data quality.

P2

Targeting Epigenetic Mechanisms As Potential Radiosensitizers In Small Cell Lung Cancer

Mansi K. Aparnathi, Safa Majeed, Lifang Song, Ratheesh Subramaniam, Mary Y. Shi, Richard Marcellus, Rima Al-awar, Benjamin H. Lok

Purpose

Post-platinum-based chemotherapy, small cell lung cancer (SCLC) commonly relapses rapidly with a more aggressive chemo-resistant phenotype, which may be mediated in part by epigenetic mechanisms. The aim of this study is to identify epigenetic targets that could sensitize SCLC cells to ionizing radiation (IR). Inhibitors of lysine demethylase (KDMi, GSK-J4), histone deacetylase (HDACi, SAHA), protein arginine methyl transferase (PRMTi, MS023) and BET-Bromodomain family (BRDi, JQ1) were tested for their radiosensitizing potential.

Methods

Post-platinum-based chemotherapy, small cell lung cancer (SCLC) commonly relapses rapidly with a more aggressive chemo-resistant phenotype, which may be mediated in part by epigenetic mechanisms. The aim of this study is to identify epigenetic targets that could sensitize SCLC cells to ionizing radiation (IR). Inhibitors of lysine demethylase (KDMi, GSK-J4), histone deacetylase (HDACi, SAHA), protein arginine methyl transferase (PRMTi, MS023) and BET-Bromodomain family (BRDi, JQ1) were tested for their radiosensitizing potential.

Results

(i) Epigenetic monotherapy: All 10 cell lines were responsive to GSK-J4 and SAHA with IC50 as low

as 3 μ M. Other interesting epi-probe, JQ1 was effective on 9/10 cell lines with a broader range of IC50 from 5.7 μ M to 150 nM. MS023 demonstrated lesser universal potency. (ii) IR monotherapy: All 10 cell lines demonstrated a broad spectrum of sensitivities to 4 days of IR and are ranked from most to least radiosensitive: H446, H82, SHP77, JHU-LX22cl, H889, H1092, H196, H69, SBC5, H526. (iii) Epi-probes + IR combination therapy: JQ1, SAHA, GSK-J4 and MS023 significantly radiosensitized 6, 5, 4 and 4 cell lines respectively. Although JQ1, SAHA and GSK-J4 demonstrated universal potency as a single agent in most of the cell lines, radiosensitization in the same cell lines was not universal. On the contrary, MS023 was not effective as monotherapy, yet it demonstrated ability to radiosensitize 4 cell lines. H82 is a sensitive cell line which was radiosensitized by all epi-probes used.

Conclusion

These results show that treating cells with IR in conjunction with epigenetic modifiers may potentially improve therapeutic efficacy of radiotherapy in SCLC. Further validation is being done with long term colonogenic assays and in vivo studies for the potent radiosensitizing candidate drugs. Ongoing work to identify biomarkers of radiosensitization by an epi-probe is planned.

P3

Response And Intervention To Elevated ESAS Scores: A Chart Audit Of Gynecologic Oncology Clinics

Soha Atallah Jackie Bender Anthony Fyles Kathy Han Michael Milosevic Sarah E. Ferguson Stephanie L'heureux Zihui Amy Liu Jennifer Croke

Purpose

While the incorporation of patient-reported outcomes (PROs) in oncology has several benefits, data pertaining to symptom management practices are limited. The objective of this study was to evaluate health care professional (HCP) documentation of elevated PRO symptom scores and subsequent intervention.

Methods

This was a retrospective chart review of gynecologic oncology patients within a single institution. The Edmonton Symptom Assessment System (revised version) (ESAS-r) is a validated, PRO tool that evaluates 9 common symptoms and is completed prior to each clinic visit. Symptom management intervention guidelines exist for each symptoms based on severity: mild (1-3), moderate (4-6) and severe (≥ 7). Biopsy-proven gynecologic oncology patients with any ESAS symptom score ≥ 4 were eligible. A stratified sampling method was used: 100 patients were randomly selected with 20 per year from 2012 to 2016. Patient, tumor and treatment characteristics were collected. HCP documentation of symptoms with score ≥ 4 and subsequent interventions were assessed by 2 independent oncologists. Interventions were categorized as: counselling, investigation, treatment or referral. Descriptive statistics were used to report symptom prevalence, HCP documented response and intervention. Fisher's exact test evaluated documentation and intervention rates according to individual symptom severity and total ESAS score.

Results

Between January 2012 and December 2016, a total of 5849 patients completed the ESAS. Symptoms scores were ≥ 4 in 3216 patients (55%) and > 7 in 1446 (25%). In our sample of 100, ovarian malignancies were most common (42%), followed by endometrial (34%). Median age was 55 years (range 47-63). The median total ESAS score was 24 (range: 17-39). The most prevalent symptoms were tiredness (70%), anxiety (61%) and poor appetite (40%). Overall, documentation of a least one symptom ≥ 4 occurred in 50 patients (50%), most commonly for pain (71%) and tiredness (36%) and least commonly for depression (11%) and nausea (4%). An intervention was offered to only 32 patients (32%), most commonly for pain (56%) and least commonly for nausea (4%). The primary intervention was a treatment recommendation (12/32; 38%). Higher median total ESAS score was associated with higher rate of documentation ($p=0.002$) and higher rate of intervention ($p<0.001$). Similarly, higher symptom severity was significantly associated with higher rate of documentation, except for anxiety and nausea, and higher rate of intervention, except for anxiety, nausea and tiredness.

Conclusion

A significant proportion of gynecologic oncology patients report elevated symptom scores that should prompt an intervention. However, HCPs document symptoms in only half of patients and offer interventions in only one third, warranting further evaluation. A study exploring the barriers and facilitators of optimal ESAS use is underway.

P4

Outcomes Of Oral Cavity Squamous Cell Carcinoma Patients Under The Age Of 40 Years: A Propensity Score Matched Analysis

Astrid Billfalk Kelly, Shao Hui Huang, Wei Xu , Lu Lin, Raymond Wu, Andrew Bayley, Scott Bratman, John Cho, Meredith Giuliani, John Kim, Brian O'Sullivan, Jolie Ringash, Aaron Hansen, Jonathan Irish, Eric Monteiro, John de Almeida, David Goldstein, John Waldron, Andrew Hope, Ali Hosni

Purpose

Conflicting evidence exists regarding prognosis in younger patients with oral cavity squamous cell carcinoma (OSCC) compared to older counterparts. We compared the outcomes of OSCC patients <40 year-old (yo) to those between 40-70 yo treated at our institution.

Methods

All OSCC treated between 2005-2017 were reviewed. Clinical characteristics and outcomes of a younger cohort (age <40 yo) were compared to the all the older (40-70 yo) patients, and then to a 1:1 matched propensity score matched older cohort. The cohorts were matched including: gender, ECOG performance status (PS), pT- and pN-categories, primary tumor subsite (oral tongue vs other subsites), resection margin status, and presence of extranodal extension (ENE). The primary endpoint was 5-yr overall survival (OS, measured by Kaplan-Meier method), and secondary endpoints were 5-yr locoregional failure (LRF, analyzed by competing risk method), and disease-free survival (DFS, evaluated by Kaplan-Meier method).

Results

A total of 57 patients were identified in the younger (< 40) cohort which had a median follow up of 4.3 (0.1-13.6) years, and 441 in the older (40-70) cohort who had a median follow up of 2.7 (0.2-9.4) years. Among the younger (< 40 yo) cohort: median age was 33 yo, 24 (42%) females, 35 (61%) non-smokers, and 25 (44%) non-drinkers; bilateral and ipsilateral neck dissection

was performed in 12 (21%) and in 30 (53%), respectively. Postoperative radiation therapy was given in 23 (40%), and concurrent chemotherapy in 15 (26%). Before applying the propensity score matching, a comparison of the younger cohort (n=57) and entire older cohort (n=441) showed that younger patients, had better ECOG PS (PS 0-1 98% vs 94%, p=0.022), less smoking history (37% vs 67% p=<0.01), had more oral tongue primary tumor site (81% vs 46%, p<0.001), fewer pT3-4 (18% vs 45%, p<0.001), less frequent pN+ (42% vs 65%, p<0.001), and less pENE+ (17% vs 34%, p=0.01), a similar proportion received chemotherapy (28% v 26%, p=0.76). The young patients had better 5 year OS (82% [95% CI 71%-93%] vs (66% [60-71%] p=0.008), better 5 year DFS (66% [54%-81%] vs 54% [49%-60%] p=0.031), and less LRF (26% [16%-43%]) vs 31% [27%-37%] p=0.18). Following propensity score matching (50 patients in each matched cohort); there was no significant difference between the younger and older cohort in 5-yr OS (81% [70%-94%] vs. 71% [59%-85%], p=0.18), 5-yr DFS (63% [49%-80%] vs. 64% [52%-79%], p=0.49), and 5-yr LRF (28% [17%-47 %] vs. 32% [21%-48%], p=0.29).

Conclusion

OSCC patients under 40 yo have better ECOG PS and pathologic features compared to the 40-70 yo counterparts. With propensity score matching, younger and older cohorts have comparable survival and tumor control. The clinical impression of poor outcomes for patients aged under 40yrs may represent recall bias.

P5

Evaluation of Partial Breast Irradiation Suitability In Early Stage Breast Cancer Patients

Gemma Corey, Anne Koch, Kathy Han, Grace Lee, Tom Purdie, Chris McIntosh, Fei-Fei Liu, Anthony Fyles, Wilfred Levin, Jenn Croke, Tatiana Conrad, Danielle Rodin, Aisling Barry, Nhu Tram Nguyen

Purpose

Partial Breast Irradiation (PBI) treats the tumour bed plus a margin in low risk early stage breast cancers, reducing exposure to organs at risk. Randomised trials have shown that PBI with external beam radiotherapy is non-inferior to whole breast irradiation (WBI) in terms of local control with fewer late normal tissue adverse events. We aimed to determine the proportion of women with early stage breast cancer suitable for external beam PBI at our institution using adapted ASTRO acceptability guidelines for accelerated PBI.

Methods

Patients were identified retrospectively from January 1, 2013 to November 1, 2018 based on age (≥ 55), tumour size (≤ 2 cm invasive, ≤ 2.5 cm DCIS), nodal negativity and grade (1 or 2). Cases identified were unifocal, LVI negative, ER+ve, HER2-ve, with margins ≥ 2 mm (invasive) and ≥ 3 mm (DCIS), no chemotherapy, non-lobular, no EIC, no previous/ bilateral cancers and endocrine therapy optional. Planning scans were reviewed to assess surgical clips and determine cavity visualisation scores (CVS); CVS 1=cavity not visualised, CVS 2=cavity visualised with indistinct margins, CVS 3=cavity visualised with some distinct margins and heterogeneous appearance, CVS 4= cavity visualised with mostly distinct margins and mildly heterogeneous appearance, CVS 5=all cavity margins clearly defined and homogeneous appearance.

Results

Thirty-seven percent (1051/2824pts) of cases identified were deemed eligible based on age, grade and T1N0/Tis. Of the 1051, 306 (29%) met all the pathologic criteria (main reasons for exclusion: previous breast cancer, lobular histology, or multifocality). Median age of eligible cases was 65 years (range 55-88yrs). The majority (254pts) had invasive disease (T1mi: 6, T1a: 17, T1b: 98, T1c: 133); 52 had DCIS. There were 169 right-sided and 137 left-sided cases. Endocrine therapy was documented in 55% of cases. CVS (1-5) were: 11%, 22%, 30%, 29%, 8%. Overall, sixty six percent (201/306) of cases were considered suitable for PBI radiologically (of the 201 cases 97% had CVS ≥ 3). Seventy two cases (72/306; 24%) had tumour bed clips, of which, 34 were considered suitable for PBI (91% -CVS ≥ 3 , 9%- CVS 2).

Conclusion

Overall, a low proportion of all patients were eligible but a high proportion of eligible cases in this cohort were suitable for PBI based on CVS score and/ or surgical clip placement. However, suitability for PBI within the cohort with surgical clips was low. Visualization of the tumour bed is essential to safely deliver PBI and is guided by identification of the cavity seroma and/ or surgical clips. Development of standard practice guidelines for surgical clip positioning to identify the tumour bed will potentially assist in increasing the proportion of early stage breast cancer patients suitable to receive PBI, even if the CVS is less favourable.

P6

Construction And Evaluation Of Novel Water Calorimeter For Use In An MR-LINAC

Mark D'Souza Humza Nusrat James Renaud Gerrard Peterson Niloufar Entezari Arman Sarfehnia

Purpose

Water calorimetry is a standard method for obtaining absolute dose-to-water measurements. In it, absorbed dose is determined by measuring the radiation induced temperature change in water. Advancements in image-guided radiotherapy have yielded an MR-integrated linear accelerator (1.5T, 7MV). In the presence of a magnetic field, electrons experience the Lorentz force and therefore have a different dosimetric impact. This effect must be corrected for in ion chambers, which are typically used in clinical settings. We aim to construct a MR-compatible water calorimeter that can accurately measure dose-to-water and be used to calibrate other detectors.

Methods

Finite Element Method (FEM) software (COMSOL Multiphysics 5.3a) was used to optimize calorimeter design. To eliminate convection, the calorimeter was designed to run at 4 °C. Different insulators (Cryogel, air, and styrofoam) and wall thicknesses for the exterior of the calorimeter tank were simulated to minimize non-radiation temperature fluctuations within the calorimeter. A glass vessel filled with high purity water surrounds the point of measurement to minimize radiation-induced chemical changes. Temperature change is measured with thermistors whose electronic resistance changes with temperature. FEM analysis was used to minimize heat conduction and beam perturbation at the point of measurement by optimizing the glass vessel's dimensions (height, radius, and thickness) for photon and electron beams. Beams were simulated using Monte Carlo methods

(GEANT4.10.3). Construction of the calorimeter was performed using plastic and ceramic components ensuring MR-compatibility and allowing it to be imaged using MR/KV imaging. Measurements were taken in a conventional Elekta Agility LINAC as well as in an Elekta MR-LINAC in the absence of a magnetic field. These results were compared to an NRC calibrated A1SL ion chamber.

Results

For the exterior of the calorimeter a three-shell acrylic system with Cryogel provided the best insulation. This system provided resistance against temperature fluctuations of up to 2 °C. The lid of the calorimeter was designed with a beam window, hydraulically driven stirrers, and passages for coolant to flow through. The calorimeter has a cylindrical top, a hemispherical bottom and can be operated upright and sideways. This allows for irradiation from the top with conventional/MR-linacs as well as irradiation to the sides when using volumetric and Gamma Knife delivery. Measurements showed that the beam window was a major source of heat loss. The glass vessel and thermistors contained could be seen using both MR and KV imaging. Calorimeter measurements agreed with A1SL measurements to within 2%.

Conclusion

We optimized and constructed an MR-compatible water calorimeter. It was successfully imaged using MR and KV imaging showing feasibility of positioning using imaging alone. The lid is in the process of being further insulated. Measurements in an MR-linac in the presence of a magnetic field are underway.

P7

A Retrospective Study Comparing The Allocation Of The Resources; Time, Money And Human Resource, Used For Stereotactic Radiosurgery And Whole Brain Radiation Therapy Treatment For Palliative Brain Metastases Patient At Carlo Fidani Peel Regional Cancer Center

Gaylene Medlam, Zainab Zaheer, Nawroz Fatima

Purpose

The purpose of this study is to assess the allocation of time, money and human resources for stereotactic radiosurgery verses whole brain radiation therapy for palliative brain metastases patients. The assessment will be used as a baseline for future resource allocation for the two treatment techniques.

Methods

A retrospective report will be generated of all the patients treated with SRS and WBRT since January 2015 to December 2018. From this population, 10-15 patients per year will be selected for the purpose of this study. Then through a simple comparison, the study aims to assess time, money and human resources to understand the resource allocation between the SRS treatment of single lesion, SRS treatment of multiple lesions and WBRT treatment. To satisfy the time parameter, the study will look at how much time is spent for the patient in CT simulation, treatment planning, Physics Quality Assurance, trial set-up and the actual radiation

treatment. The costs, in Canadian dollar amount, of the equipment used for SRS and WBRT treatments will also be compared. The number of staffs involved in each treatment technique will be used to assess the human resources component of the study. The data will be entered into Excel and analyzed using simple comparison of the parameters for each treatment technique.

Results

Conclusive results have yet to be obtained. Preliminary results show that SRS technique is more resource intensive in comparison to whole brain radiation therapy. Furthermore, SRS treatment of single lesion is less resource intensive in comparison to SRS treatment of multiple lesions. **This is a student project and the study is intended to be completed by April 26th, 2019**

Conclusion

Due to the study being in its preliminary results stage, it has not reached a final conclusion.

P8

Radiation-Induced, Hypoxia-Dependent Upregulation Of CXCL12/CXCR4 Signaling In Cervical Cancer

Meetakshi Gupta, Naz Chaudary, Pratibha Thapa, Richard Hill, Michael Milosevic

Purpose

The CXCL12/CXCR4 chemokine axis has been implicated in malignant progression, the development of metastases and resistance to radiotherapy (RT) and chemotherapy. Our group has previously demonstrated that RT significantly upregulates CXCL12 expression and, furthermore, that the addition of a CXCR4 inhibitor to standard radio-chemotherapy (RTCT) for cervical cancer improves primary tumor control and reduces lymph node metastases. However, the mechanism of RT-induced CXCL12 upregulation is not understood. Both CXCL12 and CXCR4 are hypoxia-regulated genes. However, we have not seen any difference in vascular density (CD31) or hypoxia (EF5) at the end of treatment to explain the increases in CXCL12 expression. Furthermore, RT has been reported to upregulate CXCL12 production in a hypoxia-independent manner. The aim of this study was to study tumor hypoxia at several time points during a course of fractionated RT and to determine if transient increases in hypoxia could be associated with upregulation of the CXCL12/CXCR4 pathway.

Methods

Primary xenografts derived directly from clinical cervical cancer biopsies were implanted in the cervixes of mice. After tracking tumor growth through repeated CT scans, the experimental arms were assigned when the tumors were 4-5 mm in size. Twenty-five mice were divided among the control (6), 10 Gy (6), 20 Gy (7) and 30 Gy (6) arms. Fractionated RT was delivered with multi-beam IMRT plans using 2 Gy daily fractions, 5 days per week, and daily image guidance. Two separate observers confirmed tumor matching on the cone beam CT scan before treatment each day. At the end of each week, the mice that had concluded the

planned treatment were euthanised along with 2 mice from the control group. Before the last RT fraction the mice were injected with pimonidazole and EF5 2 hours apart to evaluate both acute and chronic hypoxia. Immediately prior to euthanasia, Hoerscht was injected into the tail vein to evaluate tumor perfusion. The tumor was then excised and preserved for processing. Immunofluorescence staining was carried out to study tumor hypoxia, perfusion and co-localization of hypoxia with CXCR4 expression. CXCL12 gene expression was analyzed using qRT-PCR. L32 and YWAZ were used as internal control.

Results

A dose dependent increase in relative CXCL12 expression was seen during RT with a mean (\pm SD) of 0.13 (\pm 0.16) at the end of week 1, 1.45 (\pm 0.19) at week 2 and 7.26 (\pm 0.72) at the end of week 3, as compared to the control group (0.54 \pm 0.92). Immunofluorescence stains for pimonidazole (hypoxia), EF5 (hypoxia), DAPI (nuclear stain), CD31 (tumor angiogenesis), pCXCR4 (activated CXCR4 receptor) and Ly6G (myeloid derived suppressor cells) are currently being analyzed.

Conclusion

This study shows evidence of a RT dose-dependent increase in CXCL12/CXCR4 signaling that may be important in modulating treatment response through the recruitment of myeloid cell populations that, in turn, produce pro-tumoral cytokines and confer treatment resistance. The ongoing immunofluorescence studies will characterize transient, treatment-induced changes in tumor hypoxia and correlate them with CXCL12 expression. This will inform the choice and timing of biomarkers in future cervical cancer clinical trials that currently are being planned.

P9

A Retrospective Study To Determine The Efficacy Of Deep Inspiration Breath-Hold On Liver Dose And Define The Liver Dose Constraints For Right- Sided Breast Irradiation

Farimah Hadjilooei, Anne Koch, Tom Purdie, Grace Lee, Michael.Velec, Anthony Fyles

Purpose

Radiation therapy has showed clear clinical benefits for patients treated with breast conserving therapy and for patients after radical mastectomy with risk factors. The liver is one of the main organ at risk for lower thoracic tumors such as right breast, however, it is impossible to totally avoid incidental irradiation of normal organs such as liver during right breast irradiation. Unfortunately, little data is available on risk of liver damage during the right breast irradiation. A single case report in a right-sided breast cancer referred for postsurgical RT in 2015 showed an unusual large volume of normal liver tissue (134cc) in the high dose region of the tangential radiation field during the CT simulation and IMRT planning process in free breathing. Re-simulation of DIBH (Deep Inspiration Breath Hold) resulted in considerable displacement of the liver, reducing the volume of liver tissue in the target field and the mean liver dose. As there is limited data in terms of liver dosimetry and the effect of DIBH technique in right breast irradiation. Therefore it is necessary to determine the irradiated volume of liver, and effect of different techniques such as DIBH on sparing this volume in breast cancer patients. In this study we want to determine the volume of liver tissue exposure to radiation field during the right breast/chest wall radiation treatment in

right breast cancer patients, the effect of DIBH on liver dose and finally determine the liver dose constraints for right breast/ chest wall radiation treatment.

Methods

This is a retrospective cohort study and planning study. Data from 15/ Jan/ 2018 to 15/ Oct/ 2018 are collected. Approximately 150 patients with left, right or bilateral breast cancer who had CT simulation in both FB and DIBH techniques are eligible but Partial Breast Irradiation and Palliative Fractionation patients are not eligible.

Results

We hypothesized that with the use of DIBH, the volume of liver tissue in the target field decreases significantly and our preliminary result revealed significant decreasing in the volume of liver tissue in the field and mean liver dose.

Conclusion

We hypothesized that with the use of DIBH, the volume of liver tissue in the target field decreases significantly and our preliminary result revealed significant decreasing in the volume of liver tissue in the field and mean liver dose.

P10

A Survey Based Study Of Brain Metastases Management For Patients With Non-Small Cell Lung Cancers Or Melanoma

Chin Heng Fong, Natasha Leighl, Mark Doherty, Marcus Butler, David Shultz

Purpose

The purpose of our study was to assess the practice patterns of oncologists who treat patients with BrM from non-small cell lung cancer or melanoma. We also investigated the extent to which various clinical factors influence their BrM treatment decisions.

Methods

We created 2 sets of surveys: one for medical oncologists and another for radiation oncologists and neurosurgeons. Surveys were conducted online or on paper and distributed during scientific meetings. Following survey administration, data was collected, tabulated and analyzed.

Results

We hypothesized that with the advent of CNS-active targeted therapies and immunotherapies, some patients with BrM are initially managed without referral to radiation oncology or surgery. We hypothesized that oncologists are more likely to recommend systemic therapies

alone for BrM smaller than 2cm, and when patients have less than four brain lesions in total. Our preliminary result from 38 completed surveys revealed that up to 73% of medical oncologists prefer to use systemic therapies alone as the initial treatment for lung cancer patients with less than four brain lesions, all of which are less than 2cm. On the other hand, 85% of medical oncologists would refer their patients with four or more brain lesions for radiotherapy. For patients with less than four BrM, but with at least one lesion measuring more than 2cm, up to 26% would be referred for surgical resection.

Conclusion

The study is limited by the heterogeneous backgrounds of respondents, including differences in terms of access to newer systemic therapies, advanced radiotherapy treatments and neurosurgical consultations. Nonetheless, this study underscore the need for randomized controlled trials to confirm the survival benefits of systemic therapies alone as the initial treatment for patients with brain metastases.

P11

Targeting ROS Metabolism In Pancreatic Cancer In Combination With Radiation Therapy

Pallavi Jain, Azin Sayad, Erik Mollen, Michael Xie, Kevin Brown, Jason Moffat, David Hedley, Paul Boutros, Bradly Wouters, Marianne Koritzinsky

Purpose

Pancreatic cancer (PCa) is a fatal malignancy showing a 5% 5-year survival rate, creating an urgent need for new therapeutic targets. Many cancers have high production of reactive oxygen species (ROS), leaving them potentially vulnerable to targeting proteins involved in ROS metabolism. In line with this, we identified Peroxiredoxin 4 (PRDX4) as an essential gene in 26% of pancreatic cell lines by mining functional genomics datasets. PRDX4 is localized in the endoplasmic reticulum (ER) where it metabolizes H₂O₂.

Methods

We validated in nine established PCa cell lines and patient derived primary cell lines that the role of depletion of PRDX4 using siRNA or shRNA invitro and invivo. We also combined depletion of PRDX4 with Radiation therapy to determine the combinational affect invitro and invivo.

Results

In vitro depletion of PRDX4 using siRNA or shRNA leads to inhibition of proliferation and cell death in a subset of pancreatic cancer cells. This was

accompanied by increased levels of reactive oxygen species (ROS) as measured by flow cytometry. Dual-Depletion of NADPH oxidase 4 (NOX4) and PRDX4 could rescue the cell death phenotype thereby indicating that increase in ROS was a consequence of NOX4 activity. PRDX4 depletion led to focal accumulation of phosphorylated H2AX (γ H2AX) in the cellular nuclei, consistent with DNA damage. Phosphorylation of H2AX was exclusively dependent upon activation of the upstream kinase DNA-PKcs. Cells depleted for PRDX4 were also more sensitive to ionizing radiation. Depleting PRDX4 with inducible shRNA in established xenografts inhibited tumor growth.

Conclusion

This study indicates that depletion of PRDX4 causes increased ROS resulting in DNA damage leading to DNA-PKcs activation, inhibition of proliferation and cell death in a subset of pancreatic cancers. PRDX4 is a potential novel therapeutic target that may act synergistically with radiation therapy.

P12

Evaluation Of Multiparametric Magnetic Resonance Imaging Dose Painting To Dominant Intraprostatic Lesion In Prostate HDR Brachytherapy

Yannie Lai

Purpose

Prostate cancer is one of the most common malignancies affecting men. A common treatment option includes high dose rate (HDR) brachytherapy. Historically, HDR brachytherapy treatments are planned using transrectal ultrasound (TRUS) and/or computed tomography (CT) scans to deliver a uniform dose to the entire prostate. Due to the increased access to magnetic resonance imaging (MRI), HDR prostate brachytherapy are also being planned using this imaging modality. Superior soft tissue contrast is observed with MRI thus increasing the ability to identify the dominant intraprostatic lesion (DIL) which tends to be the site of local failure. By using multiparametric MRI (mp-MRI) the DIL can be visualized to allow for a focal boost using HDR brachytherapy. The concern with this approach is the impact on dose to the adjacent organs at risks (OARs) including urethra and rectum. Dose response to DIL receiving focal boost is insufficiently documented and more research needs to be done to evaluate the safety and clinical efficacy of this technique. This study evaluates the dosimetric impact of dose escalation to the DIL and relative organs at risk. In addition, the location of recurrences, if any, will be used to evaluate the success of treatment. This research is clinically significant because it provides an opportunity for changes in practice to this large patient population. If there is significant benefit for certain groups of prostate patients to receive dose painted HDR brachytherapy to the DIL, then

this technique could change the way HDR can be delivered.

Methods

A retrospective chart audit of prostate cancer patients treated with mp-MRI dose painted HDR brachytherapy from 2014 to present at our institution will be conducted. Patient data to be collected include clinical stage, MRI stage, prostate specific antigen (PSA) levels, prostate volume, DIL location and Gleason scores. Dosimetric data collected include dosimetric information for the DIL, prostate, PTV, urethra and rectum. Biologically effective dose (BED) will be calculated to account for differences in dose and fractionations. Follow up data collected include PSA and biochemical recurrence status and recurrence location. Descriptive analysis will be performed on the data collected including mean, median, range and standard deviations. Analysis will be divided into treatment groups based on dose/fractionation schemes with each group analysed separately as well as the entire cohort a whole.

Results

Data on the following outcomes will be presented.

Conclusion

Data on the following outcomes will be presented.

P13

Quantification Of Ionization Chamber Response In 1.5 T Magnetic Field With 7 MV FFF Beam

Viktor Iakovenko, Gerard Peterson, Brian Keller, Arjun Sahgal, Arman Sarfehnia

Purpose

Reference dosimetry in magnetic resonance image-guided radiation therapy (MRgRT) systems should take into account effects of strong magnetic field on dose response of ionization chambers used for calibration and QC routines. Authors report results of experimental measurements of ionization chamber dose response as a function of angle between magnetic field direction and ionization chamber orientation.

Methods

Measurements were performed on Elekta Unity MR Linac that incorporates 1.5 T Philips magnet and a 7 MV FFF photon beam. The response of two reference-grade chambers (Exradin A19 and A1SL paired with a PTW UE electrometer) were studied. An in-house built MR-compatible water tank (28x28x35 cm) and an accompanying cylindrical insert ($r = 25$ cm) that allowed chamber rotation around cylinder axis were used. Ionization chambers were attached to the inside wall of the cylinder, and EPID on-board imaging used to verify the centre of the chamber located exactly at the MRLinac isocentre (143.5 cm, SAD). Photon source incoming from the z-direction (gantry = 0 degree) was shaped by MLC to 10x10 cm field. Ionization chamber was rotated at 20-degree increments, and resulting dose response was used to evaluate ionization chamber magnetic field corrections as a function

of angle between directions of magnetic field and central axis of the chamber.

Results

Authors have measured a clear angular dependence of dose response for both chambers. For A19, the most prominent differences were observed at 90 and 270 degrees, +4.4 % and +5.2% corrections respectively. At 90 degree ionization chamber axis was perpendicular to directions of magnetic field and photon beam, so that the Lorentz force was sweeping electron to the direction of ionization chamber tip. At 270 – electrons were swept to the stem of the chamber. For A1SL small volume chamber, we observed +0.4% at 90 and +2.6% at 270 degree. Authors have compared results with available Monte-Carlo studies, which have shown agreement well within uncertainties.

Conclusion

Reference dosimetry is a complex task in MRgRT systems; however, taking into account effects of magnetic field and identifying optimal position of ionization chamber, it becomes achievable. Methodology used in this work was successfully used to validate Monte Carlo studies performed by other groups and can be used to identify optimal orientation for other detectors used in reference dosimetry.

P14

Treatment Outcomes And Survival Following Definitive (Chemo) Radiotherapy In HPV+ Oropharynx Cancer: Largescale Comparison Of Two Population Based Cohorts

P. Lassen, S. Huang, J. Su, B. O'Sullivan, J. Waldron, M. Andersen, H. Primdahl, J. Johansen, C. A. Kristensen, E. Andersen, J. Alsner, J. Lilja-Fisher, S.V. Bratman, A. Spreafico, J. de Almeida, W. Xu, J. Overgaard

Purpose

We compared outcomes in two well-defined, population based cohorts of HPV+ oropharynx cancer (OPC) patients (pts) treated with curative (chemo) RT.

Methods

All non-metastatic HPV+ OPC treated between 2007 –2015 with definitive IMRT ± chemotherapy in two distinct cohorts were included: one was nationwide (C1) and the other institutional (C2), the latter representing one of two cancer centers within a population jurisdiction and received 80% of the region's referrals. HPV status was determined using p16-IHC staining. Outcomes were compared between the two cohorts. Actuarial rate of locoregional control (LRC), ultimate LRC (including surgical salvage), and distant control (DC), were estimated by competing risk method. Disease free survival (DFS) and overall survival (OS) were estimated using Kaplan-Meier method. Multivariable analyses (MVA) with Cox regression calculated hazard ratio (HR) adjusted for age, gender, performance status (PS), T- and N-category (8th Edition TNM), treatment schedule and smoking.

Results

A total of 1875 pts were included. C1 pts (n=1174) were treated according to nationwide guidelines: all received moderately accelerated fractionation (6fx/week), 96% (1129) received Nimorazole (a hypoxia modifier) and 73% (856) concurrent weekly Cisplatin. C2 pts (n=701) were treated according to institutional protocols: 69%

(481) received concurrent bolus Cisplatin with 5 fx/week RT, while 9% (60) and 23% (160) received 5 fx/week and 6 fx/week RT alone, respectively. No C2 pts received Nimorazole. Median follow-up was 4.8 years. Age and PS did not differ between cohorts. Compared to C2, more C1 pts were female (24% vs 16%, p<0.001), had lower T-category (T1-2: 77% vs 56%, p<0.001), N-category (N0-N1: 77% vs 66%, p<0.001), and stage group (stage I: 63% vs 44%, p<0.001), and were heavier smokers (p<0.001). Compared to C2, C1 pts had reduced actuarial probability of 5-year LRC (87% vs 93%, with adjusted HR by MVA=0.47 [95% CI: 0.33-0.67]) and Ultimate LRC (94% vs 96%, HR=0.52 [0.33-0.82]). DC (93% vs 88%, HR=1.31 [0.95-1.82]) and DFS (81% vs 77%, HR=1.17 [0.93-1.48]) did not differ significantly between C1 and C2 cohorts, whereas OS (85% vs 80%, HR=1.29 [1.0-1.67], p=0.054) approached statistical significance. T- and N-category and chemotherapy retained independent prognostic impact for all outcomes, and heavy smoking negatively impacted LRC (HR=1.57[1.07-2.31]), DFS (HR=1.62[1.22-2.16]) and OS (HR=1.89[1.36-2.62]).

Conclusion

This pooled analysis of two population based cohorts confirms the good outcome and survival of HPV+ OPC following definitive (chemo) RT. The observed differences in RT outcomes between the cohorts probably reflect differences in treatment strategies as well as tumor and patient characteristics (including smoking status), although DFS and OS remained comparable.

P15

Synthesis And Modelling The Effects Of Dose Deposition Of The Palladium Core And Gold Shell Nanoparticle For Brachytherapy

Jason Lee, Shun Wong, Claire McCann, Carl Kumaradas

Purpose

High Z value of gold allows greater local photo-absorption followed by photoelectrons and Auger electron emission, in which, contributes to local dose enhancement. The local dose enhancement is maximized when AuNP interacts with low energy x-ray source like palladium. It has been proposed that intratumoral injection of the diffusible AuNP combined with low energy x source may enhance the dose uniformity and therapeutic dose compared to the conventional brachytherapy seeds. Purpose of this project is to test the possibility of constructing dissolvable brachytherapy seed, multi-metallic nanoparticles with a palladium-103 core and a gold shell structure and to assess its toxicity both in vitro and in vivo and to investigate the relative nanoscale dose deposition around a single palladium core gold nanoparticle.

Methods

Mono-dispersed palladium-103 core and gold nanoparticles were produced using successive reduction technique using ascorbic acid(AA) and Poly-Vinyl-Pyrrolidone (PVP). Prepared nanoparticles were characterized using TEM-EDX, UV-Vis, DLS, ICP-MS and XPS. Clonogenic assay using two cancer cell lines, MDA-231 and PC3 were used to test the cytotoxicity of nanoparticles. To assess in vivo toxicity, nanoparticles were intratumorally injected into tumor xenograft mice. Two weeks after the injection, mice were sacrificed and vital organs including liver, lung, heart, kidney, spleen and tumor were collected for histological analysis. Then we investigated the relative nanoscale dose deposition around a single palladium core gold nanoparticle (Pd-GNP) by varying the gold shell thickness and palladium core size, through

the use of a general purpose Monte Carlo code, GEANT4.

Results

as a result, cubic shaped core palladium nanoparticles with monocrystalline structure of size 18 ± 2 nm were produced and Pd-GNP showed mono-dispersed size of 50 ± 5 nm, smooth and equal thickness of gold layer and sphere shaped morphology. ICP MS found that most of injected nanoparticles stayed inside of tumour. Histological analysis showed no sign of inflammation or immune response in collected organs. This shows Pd/Au nanoparticles are highly stable and not cytotoxic in biological system. Monte carlo simulation indicate that greater and greater levels of dose deposition occur when the gold shell thickness decreases.

Conclusion

cubic shaped core palladium nanoparticles with monocrystalline structure of size 18 ± 2 nm were produced and Pd/Au NP showed mono-dispersed size of 50 ± 5 nm, smooth and equal thickness of gold layer and sphere shaped morphology. Nanoparticle were highly stable and non-cytotoxic in biological system. Based on the dosimetric study result, overall dose enhancement for this configuration might actually occur for smaller palladium sizes as well, which is indicated by the fact that the relative dose is maximized at smaller palladium and a special no gold case. This work demonstrates the feasibility of creating a dissolvable seed with Pd/Au NP, however, larger scale studies are necessary to determine if the results presented in this work lead to the conclusion that Pd-GNPs do not enhance dose if used clinically.

P16

Normal Tissue Reproducibility Using Abdominal Compression Evaluated With Magnetic Resonance Imaging

Maureen Lee, Anna Simeonov, Laura Dawson, Michael Velec

Purpose

Abdominal compression can effectively minimize respiratory motion, however, it may also introduce further anatomic variations due to inconsistencies in plate placement and the degree of compression applied. Magnetic Resonance (MR)-guided treatment systems are being developed to improve treatment accuracy. Therefore, MR-based evaluations of anatomic variability is warranted. The objective of this study is to investigate the reproducibility of normal abdominal tissues with the use of abdominal compression and visualized with MR.

Methods

This is a retrospective secondary analysis of data acquired from 20 healthy volunteers who underwent 3 MR sessions over 3 days under an abdominal compression plate device placed inferior to the xiphisternum. Volunteers were positioned head first supine, and abdominal T2-weighted axial MR was acquired followed by 2 minutes of 2D cine imaging in the sagittal and coronal planes mid-liver. Axial images were rigidly registered about the vertebra in the treatment planning system and the following structures were contoured: liver, stomach, kidneys, spleen, spinal canal and compression plate. Organ motion was quantified as the centre-of-mass difference on the 2nd and 3rd images relative to the initial image. For cine-MR datasets, respiratory motion was quantified using research software which tracks frame to frame motion of liver vessels using grey-value based 2D image registration. Daily variations in these metrics greater than 5 mm (the typical planning margin applied) were assumed to be potentially clinically relevant.

Results

The mean displacement of the liver, kidneys, canal, spleen, stomach and compression plate contours was found to be 0.36 cm, 0.30 cm, 0.08 cm, 0.35 cm, 0.81 cm and 0.79 cm, respectively. On an individual basis it was found that mean liver displacement exceeded 0.5 cm in 42.9% of the images. The 3D-vector directions for the centre-of-mass points in the above stated regions were 0.57 cm, 0.60 cm, 0.34 cm, 0.72 cm, 1.29 cm and 2.25 cm, respectively. The cine-MRI data indicates the largest magnitude of motion in the superior-inferior (SI) direction, followed by the anterior-posterior (AP) and lastly left-right (LR) with mean values of 0.59 cm, 0.56 cm and 0.11 cm, respectively. Variations in the compression plate position of more than 2 cm resulted in liver motion of >0.5 cm in 46% of cases. These variations occurred most frequently in the SI direction with a rate of 42.9%, followed by a LR displacement of 39.3% and an AP displacement of 17.8%. Stomach variations of more than 1 cm, resulted in liver displacements of >0.5 cm in 53% of cases.

Conclusion

Compression plate and stomach positioning/size variations have significant impact on daily liver displacement. More reproducible guidelines for compression plate placement and degree of compression, in conjunction with rigid dietary preparation may contribute to a reduction in these daily variations. With individual cases exceeding the liver motion tolerance of 5mm in 42.9% of the cases, more individualized and adaptive-radiotherapy techniques are warranted.

P17

Single- Institution Contemporary Results of Stage IIIA Non-Small Cell Lung Cancer (NSCLC) Treated With Radiotherapy

YQ Li ,M Meem, A Sun, A Bezzak

Purpose

Stage IIIA NSCLC is a heterogeneous group of disease with distinct prognosis, and the standard of care remains controversial. Our study is to determine the outcomes and failure patterns of stage IIIA NSCLC patients treated with radiotherapy (RT).

Methods

As a REB approved study, we retrospectively reviewed patients with pathology-proven stage IIIA NSCLC received RT from 01/2011 to 06/2016. Patients treated with upfront surgery or palliative RT were excluded from analysis. All the patients were staged with PET-CT and brain images, invasive mediastinal staging was recommended as part of initial workup. Estimates for endpoints were calculated from the time of diagnosis using the Kaplan-Meier method and compared using the log-rank test.

Results

Of 113 patients, 22, 62 and 29 were treated with radiation alone (RT), concurrent chemoradiation (ChemoRT), and preoperative chemoradiation and surgery (Trimodality), respectively. The median age is 68 years (45-87), and the most

common histology subtype is adenocarcinoma (67.3%, 76). 92% (104) of entire cohort has N2 disease and 78.8 % (89) of patients received radical dose between 60Gy to 66Gy. After a median follow-up time of 26.7mo, the median survival is 37.3mo and 3yrs overall survival (OS) is 50.3% for the entire cohort. Trimodality group has a superior 3yrs OS of 71.5% compared to 49.2 % (ChemoRT) and 14.3 % (RT alone) ($p < 0.05$). Age, smoking status and histology are not associated with OS. 36 (31.8%) patients developed local regional failure and 59 (52.2%) patients had distant failure, 28(24.7%) pts has both. Brain (12.3%) and lungs (9.7%) are the most common sites of distant failure. At 3 years, local regional recurrence rate and distant metastasis rate are 15.7% and 34.3%, 44.5% and 54.7%, 58.6% and 74.6% for trimodality, ChemoRT and RT alone, respectively.

Conclusion

In our center, maximal locoregional control with trimodality in well selected IIIA NSCLC patients is associated with superior local regional control rate, distant control rate and overall survival. Distant failure is the main type of failure in trimodality group.

P18

Features Of Patients Living Less Than 3 Months Following Spine Stereotactic Body Radiotherapy

K. Liang Zeng, Chia-Lin Tseng, Sten Myrehaug, Hany Soliman, Zain Husain, Arjun Sahgal

Purpose

Stereotactic body radiotherapy (SBRT) to the spine offers superior local control and potentially pain relief compared to conventional radiotherapy. Patients with longer survival realize these benefits most, and physician prognostication is historically poor. The purpose of this study was to report factors associated with < 3-month survival after spine SBRT.

Methods

A prospective database of consecutive patients treated with spine SBRT between 2009 and 2017 was reviewed. Dates of death were obtained through institutional records and obituaries.

Results

A total of 21 of 230 patients (9.1%) passed away within 3 months of starting treatment representing 48 total spinal segments treated. There were three deaths (14.3%) related to progression of spinal disease. The median survival and age were 56 days (range: 14-79 days) and 61 years (range: 29-85 years), respectively. The most common indications for SBRT were retreatment (n=8, 38.1%) and de novo metastases (n=8, 38.1%), followed by post-operative SBRT (n=5, 23.8%). Median time from cancer diagnosis to spine SBRT was 20 months

(range: 0.9-116 months). Most patients were ECOG 0 or 1 (n=14, 66.7%) and had no neurologic deficits (n=17; 81.0%). Lung (n=7, 33.3%) and renal cell carcinoma (n=6, 28.6%) were most common primary cancers and 7 patients (33.3%) had oligometastatic disease. Most patients had other sites of visceral metastases to sites such as the liver, lung or brain (n=17, 81.0%). Many had epidural (n=10, 47.6%) and/or paraspinal extension of spinal disease (n=12, 57.1%). 13 patients (61.9%) had SINS potentially unstable or unstable lesions. In 27 segments evaluable with follow-up imaging, 4 (14.8%) had radiologically progressed prior to death.

Conclusion

We report excellent patient selection in those who receive spine SBRT. Patients who passed away < 3 months after SBRT were heavily pretreated, with 62% of patients having had surgery or prior radiotherapy to the same spinal segments. A relatively large proportion of patients with visceral disease burden and paraspinal and epidural spinal disease died < 3 months after treatment. Further work to elucidate factors associated with poor survival are needed to further identify patients who will benefit most from spine SBRT.

P19

Opioid Consumption And Pain In Gynecological Cancer Patients That Underwent Spinal Anesthesia For Interstitial Brachytherapy

Gordon Locke, Lucas Mendez, Amandeep Taggar, Toni Barnes, Stephen Choi, Laura D'Alimonte, Eric Leung

Purpose

Brachytherapy is an essential component of many gynecologic malignancies. Interstitial Brachytherapy (ISBT) is an effective option for delivering conformal high dose radiation to the target volume with better organ-at risk sparing. However, ISBT is associated with increased pain due to implantation of multiple needles and patients require anesthetic at the time of insertion. At our institution, anesthesia protocol was changed from general anesthesia (GA) to spinal in September 2017 due to workflow requirements. This study's objective was to look at pain levels and opioid consumption in the first cohort of patients who underwent spinal anesthesia for ISBT and compare with our previous cohort of patients that underwent GA.

Methods

The first 26 patients that underwent spinal anesthesia for ISBT from September 2017 to July 2018 were analyzed from a prospective institutional database. Mean age of the patients was 62. Primary diseases consisted of 15 cervical cancers, 6 recurrent endometrial, 3 vaginal and 2 others. Baseline patient characteristics, radiation treatment details, anesthesia records and inpatient charts were obtained. Opioid consumption was quantified as oral morphine equivalent per day (OMEq/day) from postimplant until template and needles removal. Pain score levels were collected by using an 11-point scoring system, numerical rating scales (NRS). Pain and opioid consumption were

compared with a previously analyzed cohort of 48 patients in the same database who underwent ISBT with GA.

Results

Of the 26 patients, 17 patients underwent a second ISBT insertion with spinal anesthesia. 12 patients required parenteral opioid analgesia post implant. No difference in OMEq/day or pain scores was seen between admissions (mean consumption 41.4mg and 48.6mg, $p=0.64$, median interquartile range pain scores 5, [2.75-7.75] vs 4, [2-7], $p=0.35$). Patients who received IV opioids used larger amounts of opioids than patients with oral opioids (OMEq/day 69.7 mg vs 17 mg, $p=0.04$). Compared to a previous cohort of patients at our institution who underwent ISBT with GA, a significantly lower OMEq/day was noticed across all admission (44.1mg vs 65.2mg $p=0.02$) with spinal. There was no difference in intensity of the reported pain. Peak pain scores were seen in the evening with spinal compared to immediately following the insertion in the GA cohort.

Conclusion

In patients undergoing ISBT with spinal anesthetic, pain can be managed with oral analgesics in the majority of patients. Peak pain scores after the procedure are delayed in patients with spinal when compared to GA. Patients had similar levels of reported pain across cohorts however opioid use was lower in the spinal cohort as compared with GA cohort.

P20

Evaluation Of Dosimetric Predictors Of Acute And Late Toxicity After IMRT With Concurrent Chemotherapy For Anal Cancer

Jelena Lukovic, Ali Hosni, Amy Liu, Jasmine Chen, Tony Tadic, Tirth Patel, James Brierley, Rebecca Wong, Jolie Ringash, Laura Dawson, John Kim

Purpose

To evaluate the impact of dosimetric parameters on acute and late toxicity for patients with anal canal squamous cell carcinoma treated with image-guided intensity modulated radiation therapy (IG-IMRT) and concurrent chemotherapy. A prospective cohort of patients treated with institutional standardized target and organs-at-risk (OAR) contouring, planning and image-guided treatment delivery provided an opportunity for refinement of current dose-volume tolerances for OARs.

Methods

Patients were enrolled in a prospective cohort study between 2008 and 2013. Curative intent radiotherapy consisted of 27Gy/15f- 36Gy/20f to elective targets and 45Gy/25f - 63Gy/35f to gross targets. Dose selection was based on tumor clinico-pathologic features. The chemotherapy regimen was 5-fluorouracil and mitomycin C (weeks 1&5). OARs were contoured according to institutional standards and subject to peer review. Toxicity was graded using NCI CTCAE v.3. QOL was assessed with the EORTC QLQ-C30 and CR29 questionnaires. Logistic regression was used to assess the association between each dose volume parameter in turn with acute and late grade 2+ and grade 3+

toxicities. Predictive risk of normal tissue complications was calculated for each patient.

Results

Of the 101 patients enrolled in the cohort study, 87 and 79 patients were included in the acute and late toxicity analyses, respectively. The median follow-up was 3.43 years (range: 2.67-4.69 years), 42 (48.3%) of patients were male, 30 (34.5%) had T3/4 category tumors, and 32 (36.7%) had node positive disease. Median radiation dose was 63Gy. Several dose-volume parameters that are statistically significant for organ-toxicity were found. Most patients had G2+ diarrhea with small increments in irradiated volume substantially increasing the risk. Maximum point dose (Dmax) was also predictive of acute diarrhea. Skin toxicity occurred at a low doses and there was a linear increment in risk of toxicity with dose. Skin Dmax was also predictive of acute skin toxicity. Less than 15% of patients experienced acute G2+ nausea and vomiting.

Conclusion

In this initial evaluation, statistically significant dose-volume limits were identified for acute and late toxicity. Validation of the results is required and is ongoing.

P21

Assessment Of TAK-243 As A Novel Therapeutic For Small Cell Lung Cancer

Safa Majeed, Mansi Aparnathi, Lifang Song, Jessica Weiss, Aaron Schimmer, Ming Tsao, Geoffrey Liu, and Benjamin Lok

Purpose

Small cell lung cancer (SCLC) is an aggressive disease that accounts for ~15-17% of lung cancers[1], with a dismal overall five-year survival of 7%[2]. The current standard of care prescribes a first-line therapy of chemotherapy+/-radiation, which has remained the same over the past 20 years[3]. TAK-243, an irreversible inhibitor of the ubiquitin activating enzyme (UAE) E1, holds promise as a novel SCLC therapy. TAK-243 dysregulates many cellular processes, including DNA repair signalling and protein degradation by impairing the ubiquitin conjugation pathway[4,5]. Thus, by dysregulating cancer-specific dependencies of UAE, TAK-243 may induce malignant cell death[4,6–8]. Hyer et al. discovered that TAK-243 is particularly effective for 2 SCLC cell-lines, compared to a variety of other cancer and normal tissues (n=31)[5]. However, TAK-243 has not been evaluated as monotherapy or in combination with standard chemotherapy for SCLC.

Methods

The efficacy of TAK-243 as a single agent was assessed in a subset of variant and classical SCLC cell-lines. Cell-lines were treated with incremental doses of TAK243 (0-1uM) and cell viability was determined using a resazurin conversion assay after 5 days to determine EC50 values. To evaluate combination chemotherapy, cisplatin and etoposide (C/E) were administered (1:1 ratio, 0-1uM) to cell-lines together with

TAK243 at cell-line specific doses yielding 30-35% kill by TAK-243 alone. EC50 values were compared between TAK-243+chemotherapy and chemotherapy alone groups using the Extra Sum-Of-Squares F Test.

Results

Single-agent therapy. TAK-243 monotherapy elicited a range of responses in SCLC cell-lines after 5 hours. EC50 values of evaluated cell-lines ranged from 1nM to 2750nM for NCI-H146, NCI-H69, NCI-H446, SBC-5, NCI-H196, NCI-H889, NCI-H1963 and NCI-H526, respectively. Combination therapy. TAK-243 treatment with C/E revealed Δ EC50 values ranging from 0-10nM. NCI-H889 demonstrated chemosensitivity to combination treatment, with a significant change in EC50 ($p < 0.0001$) compared to treatment with chemotherapy alone. However, TAK-243 appeared to elicit additive effects with C/E in other cell-lines.

Conclusion

SCLC cell-lines demonstrated a range of sensitivity to TAK-243 single agent therapy. Lower doses of CE are required for certain SCLC cell-lines when used in combination with TAK243. These preliminary findings hint that TAK243 may have the potential to improve the current SCLC standard therapies. These results are being further interrogated in vivo to determine if TAK-243 can improve radiation therapy as well for SCLC.

P22

A Multicenter Analysis Of The Utility Of MRI Based ADC Image Sets In Delineating GTVres Volumes In Cervical Brachytherapy

Kevin Martell, Kathy Han, Lucas Mendez, Elizabeth Barnes, Amandeep Taggar, Ananth Ravi, Eric Leung

Purpose

With the emergence of MRI-based brachytherapy, perineal interstitial brachytherapy (P-ISBT) has become increasingly common to deliver highly conformal doses to bulky locally advanced cervix cancers. Previous studies have shown variability between observers in delineation of gross tumor volume (GTVres) for MRI-guided brachytherapy, with conformity index (CI) of 0.58. This difference may be more pronounced when interstitial catheters are present potentially causing needle distortion and edema. Functional imaging such as apparent diffusion coefficient (ADC) map derived from diffusion weighted MRI may help increase agreement in GTVres delineation. This study hypothesized that using ADC maps to guide contouring would reduce interobserver variability in GTVres delineation in cervical cancers treated with P-ISBT.

Methods

Four cervical cancer cases treated with P-ISBT were retrospectively selected for inclusion in this study. In all cases, MR image sets including ADC maps were obtained using a single Philips scanner. For each patient, two sets of images were anonymized: one after completion of external beam radiotherapy but pre-brachytherapy (pre-BT) with a vaginal cylinder in situ and one obtained at the time of the first brachytherapy insertion (BT). Clinical stems including radiologist interpretation of the pre-external beam radiotherapy MRI scans and physical examination at the time of

brachytherapy were created to guide contouring. Four radiation oncologists from 3 centers with expertise in gynecologic brachytherapy contoured on 4 scans for each case: Pre-BT and BT T2 image sets alone, and Pre-BT and BT brachytherapy T2 image sets with ADC available to guide contouring. Kappa (K) and conformity index (CI) values were calculated between observers.

Results

The mean GTVres volume was 31 cm³. For BT contours, the mean K (0.664) and CI (0.610) showed a substantial level of inter-observer agreement. The mean pre-BT K was slightly higher (0.684), indicating increased agreement without interstitial catheters (and accompanying MRI compatible stylets) in-situ. With the addition of ADC map, the overall mean K increased from 0.668 to 0.680. However, on more detailed review, in two of the four BT cases K did not improve with the addition of ADC. These were the case with smallest mean non-ADC GTVres volume (8.5cc) and lowest K (0.491) and the case with the largest mean non-ADC GTVres volume (77.4cc) and highest K (0.777).

Conclusion

In centers with specialized expertise in P-ISBT, there is consistency between GTVres contours. However, in presence of interstitial needles, there is an increase in contour variability between observers. ADC images may help decrease this variability. Further study is warranted.

P23

Serum Cytokine Profiling As A Potential Biomarker In Intermediate Risk Prostate Cancer: An Exploratory Study

Aruz Mesci, Stanley Liu, Hans Chung

Purpose

To identify a profile of serum cytokines that may predict for biochemical failure or radiation toxicity for further study in a population of men with intermediate risk prostate cancer treated with brachytherapy.

Methods

Study population consisted of 25 men with intermediate risk prostate cancer treated with curative intent using brachytherapy plus or minus external beam radiotherapy at Sunnybrook Health Sciences Centre. Serial blood samples were collected pre-treatment, at 1 month, 6 months and 12 months post-treatment. Samples were submitted for cytokine profiling using a Bio-Plex-based human cytokine screening assay of 65 cytokines (Eve Technologies; Calgary, AB, Canada). Prostatic specific antigen (PSA) values were also recorded serially. A decrease of PSA to a value below 1.00 at 1 year has been previously suggested as an early predictor of biochemical failure, and thus,

was chosen as a surrogate of biochemical response for our study (response time). Any toxicity attributable to radiotherapy was recorded. A univariate general linear mixed model was performed to detect any associations between response time or radiation toxicity and cytokine kinetics.

Results

IL17A and CXCL10 profiles differed between patients whose PSA values declined to a value of <1.00 over less than 1 year compared to those whose response time was greater than 1 year. Similarly, IL12p40 and IL20 profiles were different between patients with documented toxicity versus those without.

Conclusion

This study identifies a number of candidate serum cytokines which show promise for further study towards establishing possible serum-based biomarkers for radiation toxicity or PSA response.

P24 **FOXO1 Inhibition as a Therapeutic Strategy for Radiation Fibrosis**

Pamela Psarianos, Xiao Zhao, Daniel De Carvalho, Kenneth Yip, Fei-Fei Liu

Purpose

Radiation fibrosis (RF) is a long-term consequence of radiation, affecting up to 70% of radiotherapy patients. The pathogenesis of this condition is complex, involving inflammatory, epigenetic, and genetic alterations which promote excessive extracellular matrix (ECM) accumulation, ultimately leading to tissue dysfunction and patient morbidity. We previously demonstrated that a shift from fatty acid oxidation (FAO) to glycolysis is a predominant and sustained alteration in RF, and that transplantation of adipose-derived stromal cells (ADSCs) can restore metabolic homeostasis while reducing fibrosis severity. We hypothesized that epigenetic regulation of metabolism may be central to the development and treatment of RF. Our objectives were to investigate DNA methylation patterns in ADSC-treated RF versus radiated control tissue to identify and target alterations specific to the reversal of RF.

Methods

Genome-wide methylation profiling was performed on the murine tissue using reduced representation bisulfite sequencing, and the HOMER motif discovery algorithm was then used to identify differentially methylated targets associated with RF reversal. FOXO1 was identified as a novel metabolic target, and its pharmacological inhibition was examined using a TGFB1-activated fibroblast model. The propensity of FOXO1 inhibition to modulate metabolism and the expression of key fibrotic

markers was assessed using Western blotting and qPCR. Finally, the therapeutic potential of FOXO1 inhibition was investigated in a murine RF model.

Results

ADSCs induced hypermethylation at the DNA binding motif of FOXO1 ($p < 0.01$). FOXO1 inhibition therapeutically restored the expression of key FAO genes ($p < 0.05$), while decreasing the expression of fibrotic proteins such as collagen and fibronectin in vitro. Furthermore, FOXO1 inhibition reduced the severity of murine skin fibrosis in vivo ($p < 0.05$). Western blotting revealed that FOXO1 may interact with the prostaglandin E2 pathway to regulate ECM expression.

Conclusion

In summary, ADSC transplantation promoted the recovery of RF, providing insight into epigenetic alterations which are specific to RF reversal. This enabled the discovery of FOXO1, a regulator of metabolism that demonstrates promise as a novel therapeutic target for RF in vitro and in vivo. Moreover, by identifying a potential convergence of the FOXO1 and prostaglandin E2 pathways, a mechanism through which FOXO1 may regulate RF has been established. Future work will include an in-depth investigation of the epigenetic regulation of key genes in these pathways. This work will lead to a deeper understanding of RF pathogenesis while proceeding toward a novel therapeutic strategy for the treatment of this condition.

P25

Dosimetric Impact of Daily Plan Adaptation for Magnetic Resonance-Guided Liver Stereotactic Body Radiotherapy

Edward Taylor, Michael Velec, Andrea Shessel, Teodor Stanescu, Laura Dawson, Daniel Letourneau, Patricia Lindsay

Purpose

Liver cancer is challenging for image-guided radiotherapy due to motion and deformation of target volumes and organs at risk (OAR), as well as the difficulty in visualizing these structures using cone-beam computed tomography (CBCT). Liver cancer patients could thus benefit significantly from magnetic resonance (MR)-guided adaptive re-planning at the time of treatment. The purpose of this work was to assess the dosimetric impact of three daily plan adaptation strategies based on daily imaging.

Methods

Three adaptation strategies were simulated for eight patients who underwent five fractions of CBCT-guided stereotactic body radiotherapy (SBRT) for primary or metastatic liver cancer: 1.) couch shifts mimicking standard guidance to match liver 2.) modification/adaptation of segment apertures to ensure coverage of lesions imaged on daily imaging, and 3.) full re-optimization based on clinical goals and daily contours. Repeat computed tomography scans for six patients for whom it was deemed necessary to replan during treatment and eight serial MR images for two study patients were used in these simulations for a total of fourteen simulated adapted plans and eight reference plans. OAR and target volume dose statistics were calculated for each plan using 2mm and 5mm PTV margins to assess the feasibility of margin reduction in the presence of daily deformations. Respiratory motion was not considered in our margins or modeled in dosimetry simulations.

Results

Plan adaptation based on segment modification to match the daily target allowed for reduction of the PTV margin to 2mm without sacrificing coverage: the percent GTV volume receiving the prescription dose was 99% versus 100% for a PTV margin of 5mm. In contrast, plan adaptation based on liver matching and couch shifts led to 86% and 90% GTV volumes receiving the prescription dose for 2 and 5 mm PTV margins. With segment modification, the mean dose to normal liver was reduced by 0.3 Gys per fraction using a 2mm PTV expansion as compared to a 5mm expansion. For all adaptation strategies, PTV margin reduction resulted in decreased non-liver normal tissue doses: using segment modification for instance, maximum dose to 0.5cc of esophagus, stomach, duodenum, and large bowel were reduced by 0.5, 0.4, 0.3, and 0.3 Gys per fraction, respectively. Full re-optimization ensured OAR dose constraints were met for all fractions; in contrast, segment modification to ensure lesion coverage resulted in OAR constraint violations in 5(3) adapted plans out of 14 using a 5(2)mm PTV margin.

Conclusion

For patients whose breathing motion can be tightly controlled, online adaptive re-planning of liver cancers based on daily MR imaging may allow for a reduction in PTV volume without sacrificing target coverage, while reducing dose to better spare normal tissues.

P26

Stereotactic Ablative Radiotherapy for Mediastinal Lymphadenopathy: A Systematic Review

Michael Tjong, Nauman Malik, Gabriel Boldt, George Li, Patrick Cheung, Ian Poon, Yee Ung, Alexander Louie

Purpose

Stereotactic ablative radiotherapy (SABR) is a form of high dose hypofractionated radiotherapy typically delivered ≤ 5 fractions and a desired BED₁₀ ≥ 100 Gy₁₀. While established for parenchymal lung tumours, its safety and effectiveness for mediastinal and hilar lymphadenopathy (MHL), is not well established, given the potential for toxicity due to proximity of nearby organs at risk. Therefore, the objective of this study was to summarize reported outcomes following SABR for MHL.

Methods

A systematic review, based on the PRISMA guidelines, was performed using MEDLINE® (PubMed®), EMBASE and Cochrane Library databases from inception until December 2018. Studies reporting outcomes from SABR specifically for MHL from all primary malignancies were included. Studies were not excluded based on SABR dosage and fractionation prescribed. Non-English studies, guidelines, reviews, non-peer reviewed correspondences, and studies with fewer than 5 patients were excluded. If multiple publications were found from the same institution, only the most recent publication and/or largest cohort were included for data abstraction.

Results

From the 223 studies initially identified, 4 studies totaling 196 unique patients met all inclusion

criteria. All studies were retrospective in design, and from single institutions. The majority (65%) of patients (n=127) had a diagnosis of non-small cell lung cancer, and breast was the second most common with 16 patients (8%). Median follow-up periods ranged between 12.0-32.2 months. SABR dose and fractionation ranged from 21 Gy to 60 Gy in 3-11 fractions, which corresponded to a median BED₁₀ ranging from 46-106 Gy₁₀. Planning tumor volume (PTV) margins employed ranged from 3 to 5 mm. Three studies reported local control (LC) rates, which were: study I) 97% (1-year) and 77% (5-year); study II) 66% (16-month) and study III) 88% (2-year). Overall survival (OS) was calculated from time of treatment in 3 studies, with a weighted median OS of 24.3 (18.0-27.2) months. Weighted progression-free survival (PFS) calculated from 2 studies were 11.4 (9.0-13.1) months. Overall, SABR was well tolerated; with a weighted Grade 3-5 toxicity rate of 6% (n = 11). The weighted treatment-related mortality (i.e. Grade 5 toxicity) rate was 2% (n=4).

Conclusion

Despite the potential for serious toxicity, SABR for MHL appears to be feasible and effective. Considering the inconsistency of reported patients, SABR prescriptions, treatments, and outcome variables, both multi-institutional and/or prospective data would be helpful to determine the relative therapeutic benefit of SABR in this high-risk treatment scenario.

P27

Well-Med: A Multidisciplinary Approach To Supporting Radiation Oncology Resident Wellness

Indu Voruganti, Barbara-Ann Millar, Ida Ackerman, Matthew Follwell, Jennifer Croke

Purpose

Wellness has emerged as an important area within post-graduate medical education. Our objective was to identify the wellness needs of radiation oncology residents in our program, and to develop a multifaceted curriculum to develop and support wellness.

Methods

Curriculum development was mapped using Kern's six-step approach. A literature review was conducted to assess the wellness landscape in postgraduate medical education, in general, and radiation oncology, specifically, and to identify gaps. Targeted needs assessments of radiation oncology residents were done in the areas of general wellness, mentorship and leadership. The results of the literature review and needs assessments were used to inform the design, development and implementation of a wellness curriculum, including goals/objectives and educational sessions.

Results

The literature review and needs assessments identified reflection, mentorship and leadership as wellness program pillars, and were combined under the name "Well-Med." For each component, educational design was undertaken and included a syllabus, lesson plan or guideline

development. For the Reflection component, a narrative medicine workshop series (n=4) was developed exploring themes of identity, work-life balance, uncertainty and creativity in oncology. The Mentorship component includes implementation of a formal mentorship program with tool development to facilitate faculty-trainee matching, mentor bios, suggested guidelines for mentorship relationships and a template for individualized career plan discussion. The Leadership component comprises key topics including interpersonal and leadership styles, teamwork, negotiation and conflict management. A leadership speaker series was initiated on some of these topics, and tailored workshops will address the remainder. Well-Med was introduced to residents in February 2019 and will be implemented in a step-wise roll-out during protected academic time.

Conclusion

We present a strategy for developing a formalized, multi-faceted program supporting radiation oncology trainee wellness. This may serve as a framework for other post-graduate training programs. Further research will include an evaluation of the curriculum and consideration for expansion to other programs.

P28

Inter-Observer Variabilities In Applicator Reconstruction And The Dosimetric Impact In HDR Gynecological Brachytherapy

Roja Zakariaee, Jette Borg, Akbar Beiki-Ardakani, Robert Weersink

Purpose

Image-guided intrauterine high-dose-rate (HDR) brachytherapy remains one of the definitive treatment modalities for cervical cancer, as recommended by GYN GEC-ESTRO Working Group. Compared to dose distributions available using standard ring and tandem applicators, addition of interstitial needles presents more conformal dose distributions. However, a non-negligible uncertainty may be present in localization of the applicator and needles on the planning images due to the planner's level of expertise, methodology, etc. This would in effect propagate to the uncertainties in the dose distribution. This study evaluates i) the inter-observer variability of ring and tandem applicator and needle reconstruction for cervical cancer treatment and ii) the dosimetric impact of this variation on OAR and target structures.

Methods

Data for five cervical cancer HDR brachytherapy cases treated with ring and tandem applicator and two interstitial catheters were used. Applicator and needle reconstruction on MR images was performed by four experts. The variability of applicator placement was evaluated by measuring the mean distance between corresponding points of the original applicator and that placed by each observer. Also, the displacement and rotation of each case relative to the original case was measured using rigid registration. The placement and length of the reconstructed needles were also evaluated. The clinical plan for each case (active dwell positions and times) was transferred onto each reconstructed model. Target and OAR EQD2 parameters commonly used in the clinical assessments were determined.

Results

The mean distance between the applicator points in the clinical case and those applied by different experts ranged between 0.1-2.1 mm. Maximum translational parameters in Left-Right, Ant-Post, and Sup-Inf directions from rigid registration of the applicators were 3.0, 2.8, and 2.0 mm, respectively. Pitch, roll, and yaw rotation angles ranged between 0.0-1.4, 0.1-4.7, and 0.1-7.5 degrees, respectively. Needle tips were on average 1.1 ± 0.6 mm apart from the clinical case. A slight indication of a pattern of shorter and longer needle lengths was observed for two of the observers. The mean difference between the target and OAR EQD2 parameters for the clinical treatment plan and those re-calculated on the four independent reconstructions was 0.3-3.3 Gy. The standard deviation of EQD2 values across five data sets was 0.3-2.6 Gy. D98 for GTV, high-risk-CTV, and intermediate-risk-CTV were at most 7.0, 5.4 and 3.0 Gy lower than the clinical plan, respectively. D2cc for sigmoid, rectum, small-bowel, and bladder were at maximum 2.6, 2.4, 2.5, and 3.9 Gy larger than the clinical plan, respectively.

Conclusion

The variation of applicator and catheter reconstruction among four experts demonstrated small discrepancies within the image resolution for these treatment plans. The dosimetric impact for both target and OAR was within acceptable tolerance. However, better image quality and more standardized protocols for consistent applicator and catheter reconstruction are recommended based on this study.